NAVAL POSTGRADUATE SCHOOL
Monterey, California

THESIS

STRUCTURAL HEALTH MONITORING: NUMERICAL DAMAGE PREDICTOR FOR COMPOSITE STRUCTURES

by

Daniel L. Lannamann

March 2001

Thesis Advisor: Young W. Kwon

Approved for public release; distribution is unlimited

20010531 050

REPORT DOCUMENTATION PAGE	Form Approved OMB No. 0704-0188

Public reporting burden for this collection of information is estimated to average 1 hour per response, including the time for reviewing instruction, searching existing data sources, gathering and maintaining the data needed, and completing and reviewing the collection of information. Send comments regarding this burden estimate or any other aspect of this collection of information, including suggestions for reducing this burden, to Washington headquarters Services, Directorate for Information Operations and Reports, 1215 Jefferson Davis Highway, Suite 1204, Arlington, VA 22202-4302, and to the Office of Management and Budget, Paperwork Reduction Project (0704-0188) Washington DC 20503.

1. AGENCY USE ONLY *(Leave blank)*	2. REPORT DATE March 2001	3. REPORT TYPE AND DATES COVERED Master's Thesis

4. TITLE AND SUBTITLE: Structural Health Monitoring: Numerical Damage Predictor for Composite Structures	**5. FUNDING NUMBERS**
6. AUTHOR(S) Lannamann, Daniel L.	
7. PERFORMING ORGANIZATION NAME(S) AND ADDRESS(ES) Naval Postgraduate School Monterey, CA 93943-5000	**8. PERFORMING ORGANIZATION REPORT NUMBER**
9. SPONSORING / MONITORING AGENCY NAME(S) AND ADDRESS(ES) N/A	**10. SPONSORING / MONITORING AGENCY REPORT NUMBER**

11. SUPPLEMENTARY NOTES The views expressed in this thesis are those of the author and do not reflect the official policy or position of the Department of Defense or the U.S. Government.

12a. DISTRIBUTION / AVAILABILITY STATEMENT Approved for public release; distribution is unlimited	**12b. DISTRIBUTION CODE**

13. ABSTRACT ***(maximum 200 words)***

The use of composite materials in both civil and military applications is increasing as composites potentially offer many advantages over traditional structural materials. Composites typically provide superior strength to weight ratio, better resistance to corrosion, and especially for military applications, greater ballistic protection. Wide use of composites is found in aircraft, armored vehicles, ships and civil structures.

This present research demonstrates the ability to numerically detect damage in a composite sandwich structure using a robust non-linear finite element model (FEM). FEM techniques are used to directly represent damage and the model's response is investigated. Changes in elemental strain and strain frequency, through a Fast Fourier Transform (FFT), is evaluated. Both a cantilevered beam and a simply supported plate are studied.

14. SUBJECT TERMS Structural Health Monitoring, Finite Element Method, Composites, DYNA3D, and Non-Destructive Damage Detection	**15. NUMBER OF PAGES** 76
	16. PRICE CODE

17. SECURITY CLASSIFICATION OF REPORT	18. SECURITY CLASSIFICATION OF THIS PAGE	19. SECURITY CLASSIFICATION OF ABSTRACT	20. LIMITATION OF ABSTRACT
Unclassified	Unclassified	Unclassified	UL

NSN 7540-01-280-5500

Standard Form 298 (Rev. 2-89)
Prescribed by ANSI Std. 239-18

THIS PAGE INTENTIONALLY LEFT BLANK

Approved for public release; distribution is unlimited.

STRUCTURAL HEALTH MONITORING: NUMERICAL DAMAGE PREDICTOR FOR COMPOSITE STRUCTURES

Daniel L. Lannamann
Lieutenant, United States Navy
B.S.M.E, University of Maine, 1994

Submitted in partial fulfillment of the
requirements for the degree of

MASTER OF SCIENCE IN MECHANICAL ENGINEERING

from the

NAVAL POSTGRADUATE SCHOOL
March 2001

Author: _____
Daniel L. Lannamann

Approved by: _____
Young Kwon, Thesis Advisor

_____
Terry R. McNelley, Chairman
Department of Mechanical Engineering

THIS PAGE INTENTIONALLY LEFT BLANK

ABSTRACT

The use of composite materials in both civil and military applications has been increasing as composites potentially offer many advantages over traditional structural materials. Composites typically provide superior strength to weight ratio, better resistance to corrosion, and especially for military applications, greater ballistic protection. Wide use of composites is found in aircraft, armored vehicles, ships and civil structures.

This present research demonstrates the ability to numerically detect damage in a composite sandwich structure using a robust non-linear finite element method (FEM). The FEM is used to directly represent damage in a structure and the structure's response is investigated. Changes in elemental strains and strain frequencies, through a Fast Fourier Transform (FFT), are evaluated. Both a cantilevered beam and a simply supported plate are studied.

THIS PAGE INTENTIONALLY LEFT BLANK

TABLE OF CONTENTS

I. INTRODUCTION 1
- A. BACKGROUND 1
- B. CURRENT SHM PROJECTS AND USERS 3
- C. FOCUS OF THIS RESEARCH 5

II. LITERATURE REVIEW 9

III. FINITE ELEMENT MODELS 13
- A. CANTILEVER COMPOSITE BEAM MODEL 13
- B. SIMPLY SUPPORTED COMPOSITE PLATE MODEL 16

IV. RESULTS AND DISCUSSION 19
- A. CANTILEVER SANDWICH COMPOSITE BEAM 19
  - 1. Effects of Contact Elements 19
  - 2. Effects of Friction 19
  - 3. Mesh Density 22
  - 4. Numerical Growth 22
  - 5. Crack Detection and Prediction 23
    - *a. Case 1: Interfacial Crack between 0.24 – 0.25 meters 24*
    - *b. Case 2: Interfacial Crack between 0.0 – 0.01 meters 34*
    - *c. Case 3: Interfacial Crack between 0.01 – 0.02 meters 40*
- B. SIMPLY SUPPORTED SANDWICH COMPOSITE PLATE 47
  - 1. Effects of Contact Elements 47

V. CONCLUSIONS AND RECOMMENDATIONS 51
- A. CONCLUSIONS 51
- B. RECOMMENDATIONS 51
  - 1. Correlation 51
  - 2. FEM Plate and Cylinder geometry 51
  - 3. FEM program limitations 52

LIST OF REFERENCES 53

INITIAL DISTRIBUTION LIST 55

THIS PAGE INTENTIONALLY LEFT BLANK

LIST OF FIGURES

Figure 1. Isometric presentation of the Sandwich Beam 15
Figure 2. Case 1: Cantilever Composite Beam with Interface Crack between 0.24 - 0.25m 15
Figure 3. Case 2: Cantilever Composite beam with Interface Crack between 0.00 – 0.01m 15
Figure 4. Case 3: Cantilever Composite Beam with Interface Crack between 0.02 – 0.03m 16
Figure 5. Plane View of Composite Plate Illustrating Mesh Configuration 18
Figure 6. Comparison of Strain Plots with and without Contact Elements, First Element Left of the Left Crack Tip 20
Figure 7. Comparison of Strain Plots with and without Contact Elements Inside the Crack 20
Figure 8. Comparison of Strain Plots with and without Friction, First Element Left of the Left Crack Tip 21
Figure 9. Comparison of Strain Plots with and without Friction Inside the Crack 21
Figure 10a. Strain 0.02m Left of the Left Crack Tip, Element 588 (0.218 – 0.220m), Case 1 (0.24 – 0.25) 26
Figure 10b. PSD 0.02 m Left of the Left Crack Tip, Element 588 (0.218 – 0.220m), Case 1 (0.24 – 0.25) 26
Figure 11a. Strain 0.004m Left of the Left Crack Tip, Element 596 (0.234 – 0.236), Case 1 (0.24 – 0.25) 27
Figure 11b. PSD 0.004m Left of the Left Crack Tip, Element 596 (0.234 – 0.236), Case 1 (0.24 – 0.25) 27
Figure 12a. Strain First Element Left of the Left Crack Tip, Element 598 (0.238 – 0.240m), Case 1 (0.24 – 0.25m) 28
Figure 12b. PSD First Element Left of the Left Crack Tip, Element 598 (0.238 – 0.240m), Case 1 (0.24 – 0.25m) 28
Figure 13a. Strain at Left Crack Tip, Element 599 (0.240 – 0.242m), Case 1 (0.24 – 0.25m) 29
Figure 13b. PSD at Left Crack Tip, Element 599 (0.240 – 0.242m), Case 1 (0.24 – 0.25m) 29
Figure 14a. Strain Inside the Crack, Element 601 (0.244 – 0.246m), Case 1 (0.24 – 0.25m) 30
Figure 14b. PSD Inside the Crack, Element 601 (0.244 – 0.246m), Case 1 (0.24 – 0.25m) 30
Figure 15a. Strain at the Right Crack Tip, Element 603 (0.248 – 0.250m), Case 1 (0.24 – 0.25m) 31
Figure 15b. PSD at the Right Crack Tip, Element 603 (0.248 – 0.250m), Case 1 (0.24 – 0.25m) 31
Figure 16a. Strain First Element Right of the Right Crack Tip, Element 604 (0.250 – 0.252m), Case 1 (0.24 – 0.25m) 32
Figure 16b. PSD Strain First Element Right of the Right Crack Tip, Element 604 (0.250 – 0.252m), Case 1 (0.24 – 0.25m) 32

Figure 17a. Strain 0.02m Right of the Right Crack Tip, Element 614 (0.270 – 0.272m), Case 1 (0.24 – 0.25m) 33
Figure 17b. PSD 0.02m Right of the Right Crack Tip, Element 614 (0.270 – 0.272m), Case 1 (0.24 – 0.25m) 33
Figure 18a. Strain at the Left Crack Tip (and Clamped Support), Element 479 (0.0 – 0.002m) Case 2 (0.0 – 0.01m) 35
Figure 18b. PSD at Left Crack Tip (and Clamped Support), Element 479 (0.0 – 0.002m) Case 2 (0.0 – 0.01m) 35
Figure 19a. Strain Inside the Crack, Element 481 (0.004 – 0.006m), Case 2 (0.0 – 0.01m) 36
Figure 19b. PSD Inside the Crack, Element 481 (0.004 – 0.006m), Case 2 (0.0 –0.01m .. 36
Figure 20a. Strain First Element Right of the Right Crack Tip, Element 484 (0.01 – 0.012m) Case 2 (0.0 – 0.01m) 37
Figure 20b. PSD Strain First Element Right of the Right Crack Tip, Element 484 (0.01 – 0.012m) Case 2 (0.0 – 0.01m) 37
Figure 21a. Strain 0.024m Right of the Right Crack Tip, Element 496 (0.034 – 0.036m), Case 2 (0.0 – 0.01m) 38
Figure 21b. PSD 0.024 m Right of the Right Crack Tip, Element 496 (0.034 – 0.036m), Case 2 (0.0 – 0.01m) 38
Figure 22a. Strain 0.032 m Right of the Right Crack Tip, Element 500 (0.042 – 0.044m), Case 2 (0.0 – 0.01m) 39
Figure 22b. PSD 0.032 m Right of the Right Crack Tip, Element 500 (0.042 – 0.044m), Case 2 (0.0 – 0.01m) 39
Figure 23a. Strain First Element Left of the Left Crack Tip, Element 488 (0.018 – 0.02m), Case 3 (0.02 – 0.03m) 42
Figure 23b. PSD First Element Left of the Left Crack Tip, Element 488 (0.018 – 0.02m), Case 3 (0.02 – 0.03m) 42
Figure 24a. Strain at the Left Crack Tip, Element 489 (0.02 – 0.022m), Case 3 (0.02 – 0.03m) 43
Figure 24b. PSD at the Left Crack Tip, Element 489 (0.02 – 0.022m), Case 3 (0.02 – 0.03m) 43
Figure 25a. Strain Inside the Crack, Element 491 (0.024 – 0.026m), Case 3 (0.02 – 0.03m) 44
Figure 25b. PSD Inside the Crack, Element 491 (0.024 – 0.026m), Case 3 (0.02 – 0.03m) 44
Figure 26a. Strain at the Right Crack Tip, Element 493 (0.028 – 0.03m), Case 3 (0.02 – 0.03m) 45
Figure 26b. PSD at the Right Crack Tip, Element 493 (0.028 – 0.03m), Case 3 (0.02 – 0.03m) 45
Figure 27a. Strain 0.004m Right of the Right Crack Tip, Element 596 (0.234 – 0.236m), Case 3 (0.02 – 0.03m) 46
Figure 27b. PSD 0.004 m Right of the Right Crack Tip, Element 596 (0.234 – 0.236m), Case 3 (0.02 – 0.03m) 46
Figure 28. Center Displacement Divergence of the Plate with 0.01m by 0.01m Interfacial Crack with Contact Elements and Zero Friction 48

Figure 29. Load Point Displacement Divergence of the Plate with 0.01m by 0.01m Interfacial Crack with Contact Elements and Zero Friction 48
Figure 30. Center Displacement of the Plate with 0.03m by 0.03m Interfacial Crack but without Contact Elements 49

THIS PAGE INTENTIONALLY LEFT BLANK

LIST OF TABLES

Table 1. Material Properties of the Composite Beam and Plate 13
Table 2. Crack Coordinates for the Composite Plate 17
Table 3. Case 1 FEM Interface Crack Detection Results 24
Table 4. Case 2 FEM Interface Crack Detection Results 34
Table 5. Case 3 FEM Interface Crack Detection Results 41

THIS PAGE INTENTIONALLY LEFT BLANK

ACKNOWLEDGMENTS

I would like to thank Dr. Young Kwon whose guidance and direction made the completion of this thesis research possible. I would also like to thank LTJG Johannes Jolly, USN, for his assistance in learning the UNIX® operating system and the modeling software DYNA3D. Additional thanks go to LT Rick Trevisan, USN, who created the AutoCAD® pictures. Ms. Theresa Pham provided me with moral support in addition to developing the MATLAB® Fast Fourier Transform routines. I am eternally indebted to my parents and family for all that they have done for me throughout my life. Of course, none of this would have been possible or even desirable if not for the support, patience and unconditional love of my dear wife, Kelly. Most importantly, I want to thank the Blessed Trinity and my Holy Mother Mary for helping me through out this process. I thank Saint Jude for his intercessions to God on my behalf.

THIS PAGE INTENTIONALLY LEFT BLANK

I. INTRODUCTION

A. BACKGROUND

Approximately ten percent of America's Gross Domestic Product is consumed in the construction and maintenance of the civil infrastructure, as estimated by Helmicki, et al. (1997). Systems are designed to have service lives that span over several decades, and as such, a considerable effort is expended in structural maintenance.

Presently, damage detection methods are either visual or localized experimental methods such as radiographs, magnetic field methods, acoustic or ultra-sonic methods, eddy-current methods and thermal field methods. All of these experimental techniques require that the general vicinity of the damage is known *a priori* and that the portion of the structure being inspected is readily accessible. The time and expense of such inspections has resulted many bridges and similar structures being subject to some form of visual inspection on a biennial basis.

To address these shortcomings, Structural Health Monitoring (SHM) has become, in the last decade, a growing area of research in an attempt to more efficiently and safely address the life-cycle maintenance of such structures. SHM is also being actively investigated, tested, and used by civil and military aircraft fleets around the world to improve the expenditure of maintenance resources.

Chang (1999) estimated that the use of mature SHM systems could reduce by 40 percent the time spent performing fighter aircraft inspections, which for the F-18 series aircraft translates to over 35 million dollars per year. Foote (1999) reported that the consortium designing and building the Eurofighter was intent on including an expansive,

fiber-optic strain gauge based SHM system to provide for real-time aircraft structural fatigue monitoring.

The ability to have real time knowledge of the health of an in-service structure is a major objective for structural engineers, maintenance crews, and manufacturers. This ability will allow better scheduling of routine and corrective maintenance, failure prevention, and cheaper, more efficient manufacturing.

All of this potentially leads to a more productive use of the structure and a reduced life-cycle cost. A fundamental requirement of such a passive system would be a detailed knowledge of the actual in service loading conditions of the structure. In much broader terms, Chang (1999) went on to outline the future requirements and potential beneficiaries of such a system, that would include, but by no means be limited to:

Aerospace - aircraft are a zero failure industry and as such are subject to extensive inspections

Military – Missile systems, aircraft, ground vehicles, and ships, for routine and damage assessments

Automobile – engine, tires, suspension and braking components

Civil Infrastructure – lifecycle monitoring of bridges, dams, roads, and buildings; for routine and post earthquake damage monitoring

The basic concept of SHM research envisions sensors that are designed for and built into a structure, such as a building, a rocket motor, or an aircraft wing. The resulting SHM system is then calibrated for its particular application, which provides the

benchmark for a healthy damage free structure, and placed into service. Then over the life of the structure, structural engineers and maintenance crews could remotely and continuously monitor the structure for damage. This would allow for real time inspection and damage evaluation. As part of his summary of the 1st International Workshop on Structural Health Monitoring, Chang (1999) detailed the potential benefits of such a passive system to include real time monitoring and reporting of structural health which would result in lower maintenance costs. Such a system would also require less direct human involvement reducing labor expenses, downtime, and human error. Another cited advantage is the automation of structural health, which improves safety and reliability.

B. CURRENT SHM PROJECTS AND USERS

Several major areas of SHM require continued research and greater development. In particular these include, sensing technology, diagnostic signal generation, signal processing, damage interpretation and identification analysis, and finally, SHM system integration.

These fundamental challenges are being addressed in many current design projects both in the US, Asia, and Europe. Designers of new structures are hampered however by the limitations of the current state of SHM systems. Not only have SHM systems typically not been optimized, many of the fundamental inputs, or sensor measuring points, have not yet been fully defined. This is often a case of not having a full knowledge, with a great deal of certainty, of just what exactly needs to be measured in a particular structure. In addition, for new designs, the added up front expenses associated with an unproven SHM system, with an uncertain payback, are often prohibitive.

While SHM systems are being included in some new designs, such as the previously mentioned Eurofighter, most current research is focused on modeling existing structures. The reasons for this are numerous. The need, especially with civil structures, is most pressing on older structures that are already in service and showing signs of age and deterioration. Additionally, civil structures are primarily static and can be investigated and instrumented easier, and with less risk than aircraft. Long term testing situations are more readily developed and modifications to the structure are either very small or non-existent. A separate challenge for researchers is locating in-service structures that they would be permitted to impose real damage on, without placing the safety of the general public in jeopardy.

A large focus of SHM research is currently concentrated on data collection and modeling of existing structures. Instrumentation of various highway and railroad bridges is building a database for future designers of just what the real loads are. Experience is also gained with various sensor types along with the toughness and reliability of these sensors in actual operating conditions. A few FEM's have been developed to serve as prediction tools and to replicate this data. It is important to note that FEM's do not exist, in any form, for a majority of structures in current use. It is equally important to bear in mind that one of the intentions of SHM is the development of such FEM's. What is intended is the modeling of basic structures and using that insight to improve SHM system integration.

The federal and several state departments of transportation, together with at least two national laboratories and other universities have ongoing projects that include various schemes of real-time monitoring of highway bridges. This approach utilizes

existing structures in an attempt to quantify both the current health of the structure and as a means to develop a database of the actual loading conditions. This data base is, as previously mentioned, a fundamental requirement for a useful SHM. Typically, these projects use empirical data to develop and refine basic finite element models. Most of these current projects are subsets of SHM, namely Non-destructive Damage Evaluation (NDE) methods, which have been categorized by Rytter (1993), are one of four types:

Level I: methods that only identify if damage has occurred;

Level II: same as Level I and simultaneously determine the location of the damage;

Level III: same as level II and provides an estimate of the damage severity;

Level IV: same as Level III and evaluates the impact of the damage on the structure.

The focus of this current research is to develop a finite element model damage predictor to support Level II NDE efforts.

C. FOCUS OF THIS RESEARCH

Historically, work in the area of global damage detection techniques has involved the use of relative shifts or changes in the modal parameters. Modal parameters such as modal frequency, modal damping, and mode shapes are a function of the mass-inertia and elastic properties of the structure. Therefore, the dynamic response of a system can be a sensitive indicator of change in the integrity of the system's elastic structure. Damage in

any form reduces the local flexural stiffness near the damage. Reduced stiffness leads to a decrease in modal frequencies and an increase modal damping coefficients as well as changes in the corresponding mode shapes. Unfortunately, as reported by Doebling (1996) most researchers have found little success in this approach to damage detection. This is because of the massive reductions in the local modulus of elasticity, required to simulate damage, provide only slight changes in the response mode shapes.

Therefore, this research has focused on an alternate approach that incorporates the robust FEM to properly model and predicts changes in the elemental strain and strain frequency of a sandwich composite structure with an interfacial crack.

The strain a structure is subjected to is directly a function of the applied load and the duration of that load. This load can have various forms, such as impact, thermal shock, or vibration. However, in the frequency domain, the shift of the response frequency is independent of both the magnitude and the duration of the applied load. As such, the FFT analysis allows for direct comparison of different loading cases. Additionally, the FFT is not dependent on a linear input and can be used to analyze nonlinear data sets.

Damage can affect the dynamic response of a structure either linearly or nonlinearly. Changes in the dynamic response of a structure subject to linear damage can be related to uniform changes in the geometry or the material properties of the structure. However, typical structural damage is predominately in the form of cracks. Such cracks behave nonlinearly under dynamic excitation as in the case where the embedded crack surfaces slide or rub against one another. The nonlinearly is due to the friction and

contact between the interfacial crack surfaces. In some nonlinear cases, the global effect of damage on the dynamic response of the structure can be considered small and local in nature. In such cases, the damage can be modeled linearly. However, in the case where the nonlinear local behavior significantly affects the global structural response, the damage can no longer be modeled linearly. This research addresses the non-linearity of the interfacial crack.

The objective of this study is to evaluate elemental strain changes near damage and whether this change could be exploited, potentially by in-situ strain gages, to detect the presence of damage in a sandwich composite structure. To this end, the present study includes an embedded crack modeled directly in the FEM instead of simulating the crack through reduced material or geometric properties. Nonlinear analysis was performed for this model to compare simple structures with and without damage. The impact of contact elements and friction were introduced in order to maximize the reality of the FEM. This thesis research focuses on the computational aspects of structural damage identification.

THIS PAGE INTENTIONALLY LEFT BLANK

II. LITERATURE REVIEW

There is quite a large amount of literature generated on global damage detection and localization by use of changes in modal parameters. The majority of literature reviewed for this research has focused on recent developments in Structural Health Monitoring (SHM). A recent and detailed summary of SHM and vibration based analysis is presented by Doebling (1996). A lot of current research continues in almost all aspects of SHM, including numerical damage predictive models, which are typically Level I and II systems. Many projects mesh empirical data into existing FEM's in an attempt to improve the FEM results and to refine the FEM's usefulness as a modeling aid and damage predictor. Both civil and military applications are expanding their use and development of SHM systems as means to improve safety, reliability, and reduce both manufacturing and maintenance costs. A brief summary of some recent selected works is outlined below.

Currently, the aerospace industry is very involved in various forms of SHM. Ikegami (1999) outlines the Boeing Company's and the U. S. Air Force's long uses of SHM systems for aging aircraft like the B-52 bomber and the KC-135 tanker. Additionally, some of Boeing's current SHM projects include the Joint Strike Fighter and the C-17 transport programs. Searle, et al (1997), outlined the use of a Broadband Acoustic Emission (BAE) system which has moved beyond the development phase for structural crack detection in the F-16 fighter. This system expected to be incorporated in the U. S. Air Force's long running Aircraft Structural Integrity Program (ASIP).

Valdiver (1997), reports on the importance and state of the U.S. Army's Missile systems health monitoring programs, especially in light of the of the recent defense draw

down with its associated reduction in the fielding new systems. This has called for improved analysis of missile components with the intent to increase service lives and reduce the need for live firing confidence checks. He also addresses the necessity to incorporate health monitoring systems in any future designs.

Other work has focused on roadway bridges. Farrar and Jauregui (1996a), Farrar et al (1996b), and Farrar and Doebling (1997) detailed how Los Alamos and Sandia National Laboratories, along with the New Mexico State University, collaborated on a project to investigate the effects of purposely installed damage in an abandoned section of Interstate 40 bridge, over the Rio Grande in Albuquerque, New Mexico. Since the bridge was earmarked for demolition, the researchers where actually permitted to impose real damage, in the form of cuts in the supporting trusses. The damage ranged in length from two and one-half to six feet. A linear, Level II, FEM was used concurrently to support this work. Additionally, the following modal based damage predictor algorithms were employed for the investigation of the health of the structure:

1. Damage Index Method
2. Mode Shape Curvature Method
3. Change in Flexibility Method
4. Change in Uniform Flexibility Shape Curvature Method
5. Change in Stiffness Method

The ability of each method to predict and evaluate damage is addressed.

Some interesting observations of these works illustrate some of the potential pitfalls of SHM systems, loading analysis, and system integration issues. More advanced plans concerning roadway issues in particular were laid out by Sikorsky (1999), who stressed the need for rapid development of Level IV systems in both aerospace and the civil infrastructure.

As the recent earthquake in Seattle, WA clearly illustrates, the need for rapid post damage evaluation of civil structures is very important of for not only public safety issues, but also economic concerns. The populace is entitled to know that the buildings that they work and live in are safe in the wake of an earthquake. For this to be a reality will require extensive Level III and Level IV SHM systems. These requirements pose very difficult problems, but the payoff is immense. For the earthquake scenario, as outlined by Mita (1999), current practice dictates the performance of very time consuming and skilled labor intensive inspections of all possible damage sites, including the possibility of non-visible damage. An effective SHM system would record the event, compare against the structures historical database, pinpoint the damage locations, and provide an evaluation of the impact of the damage on the health of the structure. This would allow structural engineers to concentrate recovery and repair efforts on buildings that have the most damage and the greatest likelihood of salvage. As would be imagined, this skilled labor force will be in very short supply following an earthquake, so the ability to efficiently maximize this asset cannot be overstated.

Lipsey (1999), in work that laid the foundation for the present study, observed that mode shape curvature was a more sensitive indicator of damage and a better locator of damage than modal frequency or mode shape displacement. Additionally, he addressed

the non-linear impact of interfacial crack surface friction, and the opening and closing of a crack in response to beam bending.

SHM is still a developing science and the literature clearly illustrates that a great deal of fundamental work remains. The focus of this research is to develop and evaluate the numerical approach to damage prediction. The offshoot of this current work, if validated by actual experimentation, would be to provide designers and operators with a valid method of damage prediction.

III. FINITE ELEMENT MODELS

The Finite Element Method has become one of the most important and useful engineering tools for engineers and scientists. This is because the FEM allows for a relatively rapid solution to very complex linear and non-linear problems. In the particular case of this research, various models of increasing mesh density were modeled in order to determine the effect of contact elements, mesh density, material properties, and friction.

A. CANTILEVER COMPOSITE BEAM MODEL

A finite element mesh representation of a sandwich composite, 0.48m long x 0.008m high x 0.04m wide, is developed as the model for the cantilever beam. The beam is subjected to a transient load at its tip and the material properties are as in Table 1.

Table 1. Material Properties of the Composite Beam and Plate

Material	Young's Modulus, N/m^2	Density, kg/m^3	Poisson's Ratio
Syntac 350C Foam	2.21×10^9	96.1	0.35
Glass Reinforced Plastic (GRP)	2.07×10^{10}	3060	0.342

In the model, Syntac 350C foam of 0.006m thickness is the core material. This is reinforced, on the top and bottom, by 0.001m thick layers of Glass Reinforced Plastic (GRP). The GRP is assumed to be a balanced and symmetric laminate, which permits modeling of the material as quasi-isotropic. The finite element model of the composite beam is as illustrated in Figures 1 through 4. An isometric view of the composite sandwich beam is presented as Figure 1. Figure 2 illustrates Case 1 where the beam has an interfacial crack located from 0.24m to 0.25m. Figure 3 and Figure 4 show Cases 2

and 3 where the interfacial cracks location as 0.0m to 0.01m and 0.02m to 0.03m, respectively. In all cases the damage, or crack, is modeled as extending through the beam width. A uniform mesh is employed to allow direct comparisons between the three crack cases. A total of 1920 nodes and 717 thick shell elements make up the model. Thick shell elements have displacements, as degrees of freedom but not rotation, like three-dimensional solid elements. The output of the FEM solves for the elemental strain at the exterior surface of the top GRP section. The laminae are modeled as perfectly joined at the interface of material types, except in the damaged section where additional nodes and contact elements are used. Three different crack location cases are presented, in each case the crack was 0.01m in length. The entire beam is modeled using DYNA3D, assuming quasi-isotropic elastic material properties. It was also assumed that no other damage was present in the beam except that which was purposely installed. In each case, the beam is subjected to a transient, uniformly distributed tip load of 50 N/m. The load is applied for 0.01 seconds and the problem analysis time is 0.24 seconds. The FEM calculates elemental strain along with tip displacement and acceleration and these results match analytical solutions. Elemental strain is plotted, using MATLAB®, versus a beam without damage where the change in elemental strain and the frequency shift, using a FFT, of elemental strain, is investigated. Note that for the beam cases, the figures show a generalized mesh. The actual mesh is too fine to clearly display the details. The bolded line represents the general location of the damage. In each case, the crack is located at the interface of the foam core and the upper GRP skin.

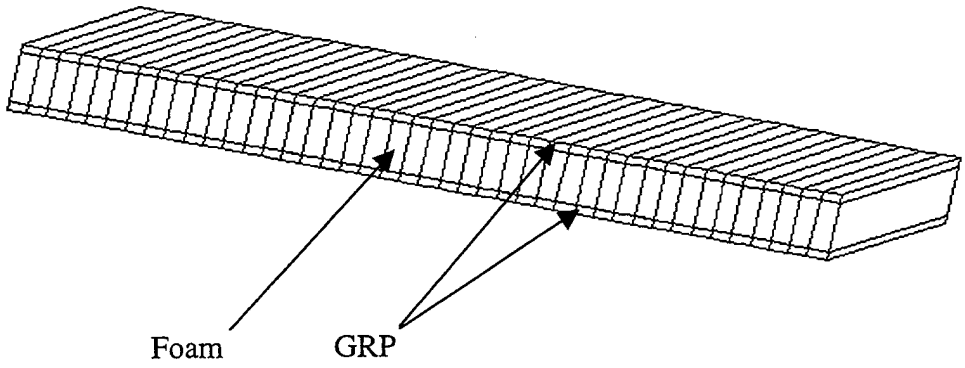

Figure 1. Isometric presentation of the Sandwich Beam

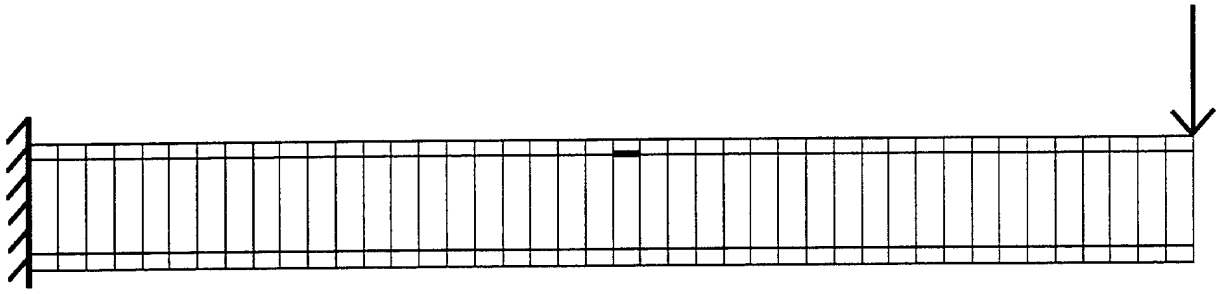

Figure 2. Case 1: Cantilever Composite Beam with Interface Crack between 0.24 - 0.25m

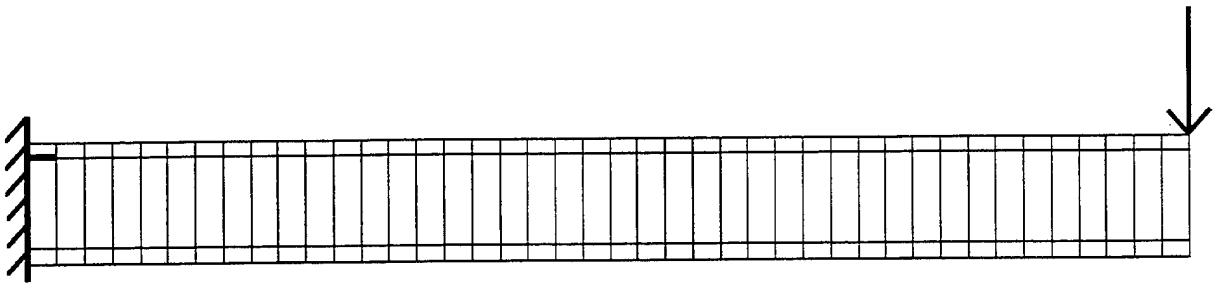

Figure 3. Case 2: Cantilever Composite beam with Interface Crack between 0.00 – 0.01m

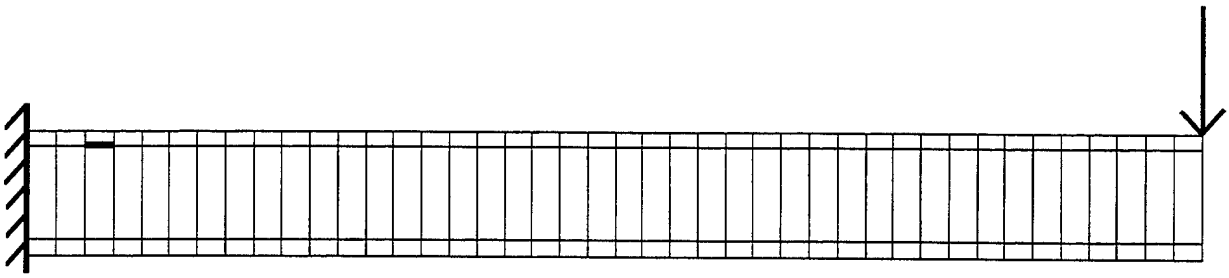

Figure 4. Case 3: Cantilever Composite Beam with Interface Crack between 0.02 – 0.03m

B. SIMPLY SUPPORTED COMPOSITE PLATE MODEL

In a similar fashion as with the cantilevered beam, a finite element mesh representation of a simply supported sandwich composite plate is developed. The same sandwich materials are used as with the beam, except now the plate measures 0.48m x 0.008m x 0.48m. Again, the plate is subjected to a transient load, which is applied away from the center of the plate. The finite element model of the composite beam is as illustrated in Figure 5. A non-uniform mesh is employed due to a hardware limitation. A total of 4900 nodes and 3464 thick shell elements make up the model. Two cases are modeled, the first has a 0.01m x 0.01m crack and the second has a 0.03m x 0.03m crack. The analysis proceeds in the same manner as the cantilever beam. An impact load of 1 Newton is applied at x = 0.27 m and z = 0.17 m. The duration of the load is 0.00125 seconds, with a problem run time of 0.025 seconds. The plate is simply supported along the edges and the dimensions and geometery of the interfacial crack is illustrated in Table 2.

Table 2. Crack Coordinates for the Composite Plate

Damage	Upper Left Pt.	Upper Right Pt.	Lower Left Pt.	Lower Right Pt.
Large Crack	0.205, 0.205	0.235, 0.205	0.205, 0.235	0.235, 0.235
Small Crack	0.205, 0.225	0.215, 0.225	0.205, 0.235	0.215, 0.235

In all cases, the model results are sampled and filtered to eliminate higher frequency components and to provide for smooth plots.

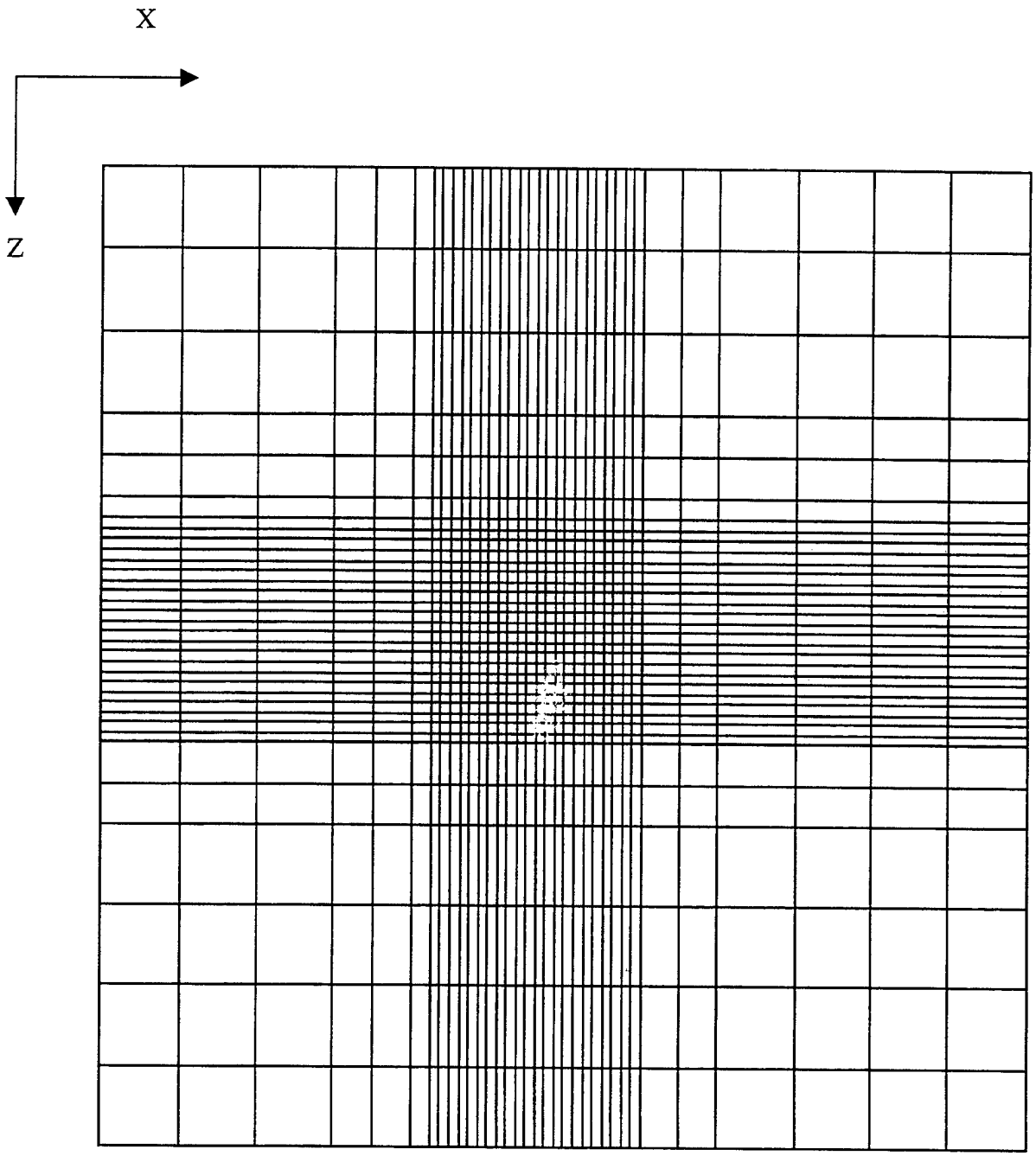

Figure 5. Plane View of Composite Plate Illustrating Mesh Configuration

IV. RESULTS AND DISCUSSION

A. CANTILEVER SANDWICH COMPOSITE BEAM

1. Effects of Contact Elements

Contact elements dampen the magnitude of the strain in damaged beams compared to models without contact elements, as illustrated in Figures 6 and 7. This is because contact elements are critical to prevent the nodes that represent the crack from overlapping each other. In other words, contact elements accurately model the opening and closing of a crack while ensuring that the nodes that constitute the crack do not slide past one another. Figures 6 and 7 show that the non-linear analyses with contact elements are important to properly represent the crack behavior.

2. Effects of Friction

The use of contact elements, in DYNA3D, also allows the modeling of friction along the crack surfaces. Actual coefficients of static and dynamic friction inside a crack are not clearly known. Values similar to ground-against-ground rubbing were modeled and the effects are detailed in Figures 8 and 9. The effect of friction was not significant. This is primarily because the crack surfaces in this case to not slide against one another, instead the crack opens and closes.

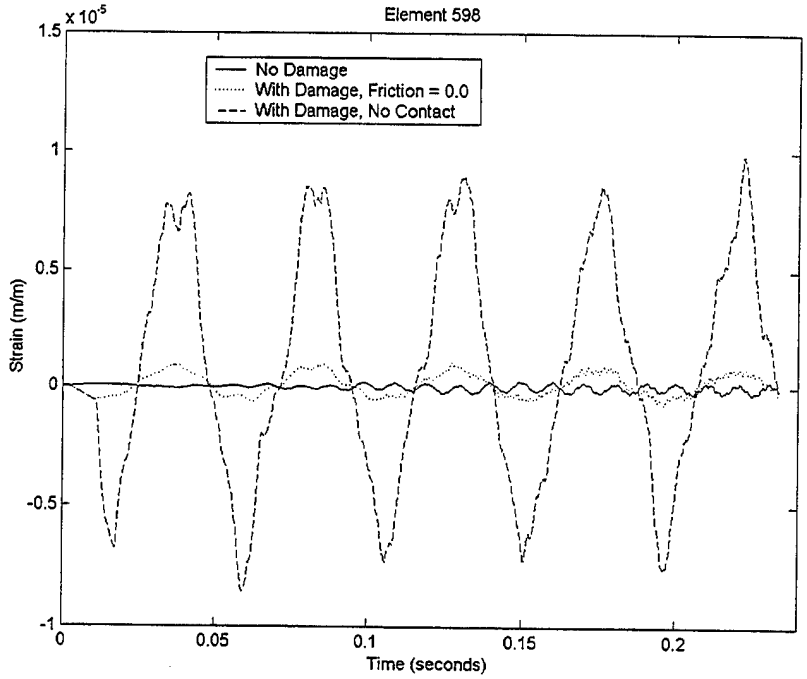

Figure 6. Comparison of Strain Plots with and without Contact Elements, First Element Left of the Left Crack Tip

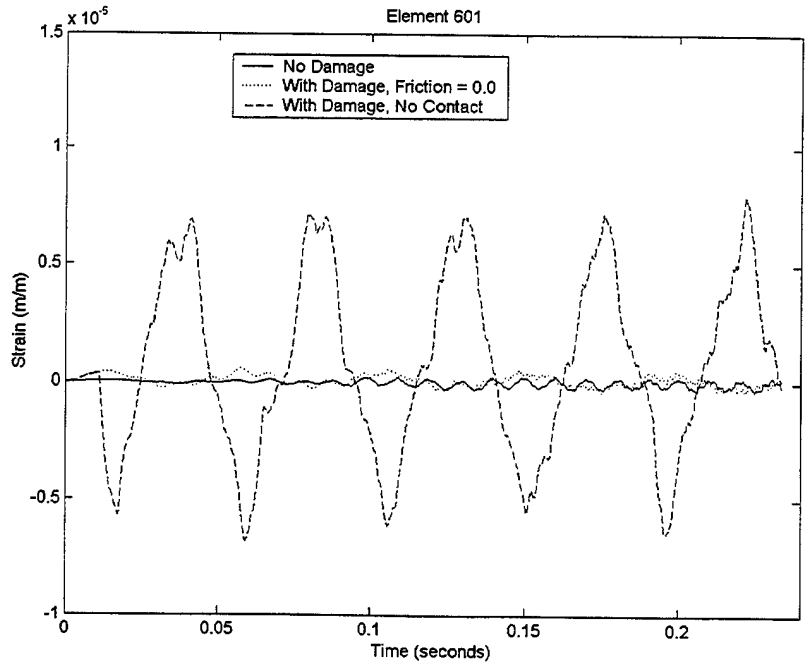

Figure 7. Comparison of Strain Plots with and without Contact Elements Inside the Crack

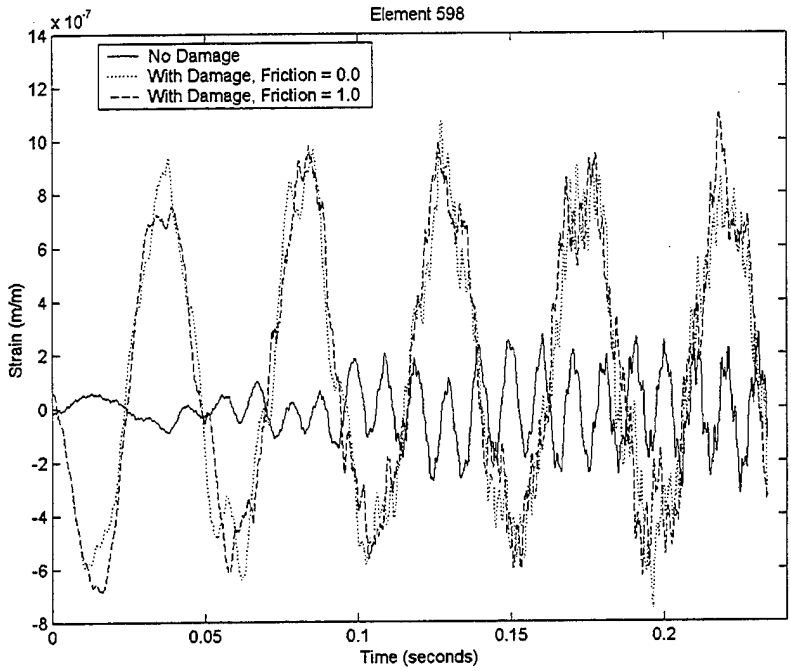

Figure 8. Comparison of Strain Plots with and without Friction, First Element Left of the Left Crack Tip

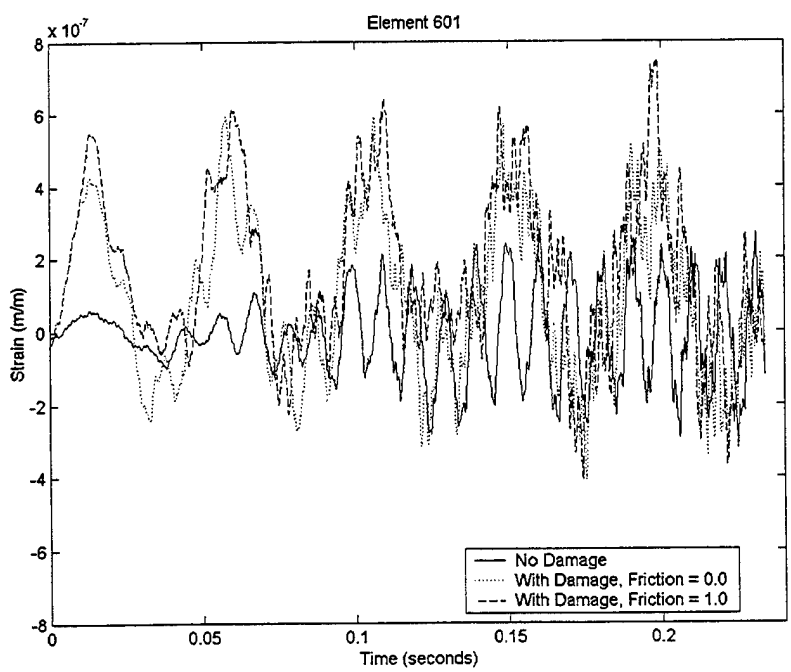

Figure 9. Comparison of Strain Plots with and without Friction Inside the Crack

3. Mesh Density

One of the underlying principles of the FEM is the ability to model structures and complex shapes using small number of large elements and obtains accurate results. However, there is a point where the model must closely match the true structure in order for each discrete element to provide accurate and correct results. This is because large numerical models are necessary to reduce discretization error in the FEM.

To have a truly robust and accurate model that is repeatable and can be used to detect and predict damage over the entire structure, this research has demonstrated the importance of having a uniform mesh density. There are several important ramifications of this requirement. Firstly, have a large number of elements, and hence a large number of nodes, in any FEM are computationally expensive. Naturally, the actual run time of the model is greatly increased; but also, the model construction time is a consideration. Secondly, in this case, a uniform mesh allows the damage to be easily "moved" within the model without the necessity of developing a new model.

4. Numerical Growth

Conversely, a fine mesh does not prevent numerical growth, which is independent of element size. Gross approximations of elemental strain may be determined by using larger elements away from the damaged section of the beam. The application of a uniform mesh of 2mm throughout the beam did not eliminate the presence of numerical growth.

Additionally, numerical growth is not a function of the Computed Scale Factor for Time step (SCFT). Reducing SCFT by half merely doubled the number of data points and did nothing to reduce the amount or presence of numerical growth.

In this particular case, the foam core appears to be a source of numerical growth. The homogeneous GRP beam model did not show instances of numerical growth. Actually, the foam core illustrates the non-linearity of the problem.

5. Crack Detection and Prediction

The intent and focus of this research was to develop a FEM that could be used to predict and localize damage in basic composite structures. To that end, a few essential observations are made.

The boundary conditions of the cantilever beam have a major impact on the FEM's ability to detect damage near the support. Regardless of the location of the damage, the beam support tends to masks the presence of damage and the effect of damage near clamped end is minimized. The dampening effect of the clamped end is seen in all cases and so large elements are useful as the first approximation of elemental strain. The important advantage of using large elements is that the resulting run time is greatly reduced. While this may seem at first like a major concern, in reality, the highest area of strain is near the structures supports and so this area is already the focus of intense scrutiny. In other words, a global SHM method is nor required demonstrating the necessity of performing NDE near the structural supports.

Three cases of composite cantilevered beams with interfacial cracks were investigated; the results of which are outlined below. Two additional examples of Case 1 were modeled to demonstrate the effect of contact elements and friction in the FEM. As noted before, the FEM solution is for the elemental strain at the top surface of the upper GRP laminate.

a. Case 1: Interfacial Crack between 0.24 – 0.25 meters

This beam is subject to a 1-cm crack originating at the center of the beam. The results of the FEM's ability to detect and localize the presence of the interfacial crack are summarized in Table 1, along with Figures 10 through 17.

Table 3. Case 1 FEM Interface Crack Detection Results

Element Location	Damage Location	Figure/Element	Detection Probability
0.218 – 0.220m	0.24 – 0.25 m	10/588	Low
0.234 – 0.236m	0.24 – 0.25 m	11/596	High
0.238 – 0.240m	0.24 – 0.25 m	12/598	High
0.240 – 0.242m	0.24 – 0.25 m	13/599	High
0.244 –0.246m	0.24 – 0.25 m	14/601	High
0.248 – 0.250m	0.24 – 0.25 m	15/603	High
0.250 – 0.252m	0.24 – 0.25 m	16/604	Low
0.270 – 0.272m	0.24 – 0.25 m	17/614	Low

The effects of the damage first appear in Element 596, Figure 11 (0.234 – 0.236m, outside the crack) as large compressive strains. This effect is seen 3 elements (0.004 m) to the left of the actual damage. The elemental strain changes from all compressive in Element 596 to a combination of compressive and tensile strains in Element 598, Figure 12. Element 599, Figure 13, (0.24 – 0.242m, which contains the left crack tip) initially shows a large compressive strain, which may be the result of the applied load, then mostly large tensile strains. This is the opposite result of the element 603, Figure 15 (right crack tip). The magnitude of element 598 (0.238-0.240m, just outside crack) is greater than any of the damaged sections. This is because of the higher bending stress the element experiences since it is closer to the clamped end and near the crack tip.

The damage is readily detectable by a sudden and dramatic increase in compressive strain in element 603, Figure 15 (0.248 – 0.250m, contains the right crack tip). Additionally, there is a noticeable increase in the magnitude of the elemental power spectral density.

The FEM does show a difference in elemental strains between the damaged and undamaged cases. Away from the damage, the effects of the damage are slight. However, when the elements near the damage are examined, the differences are dramatic. The damaged section is readily detected/predicted using a FEM. In this particular case, the FEM does an excellent job of detecting the exact range of the damage. This is because the damage is not being masked by the clamped support. The exact range of the damage would be determined by conventional means (i.e., x-ray, ultrasound, etc.). This validates the use of this method as a global predictor of damage.

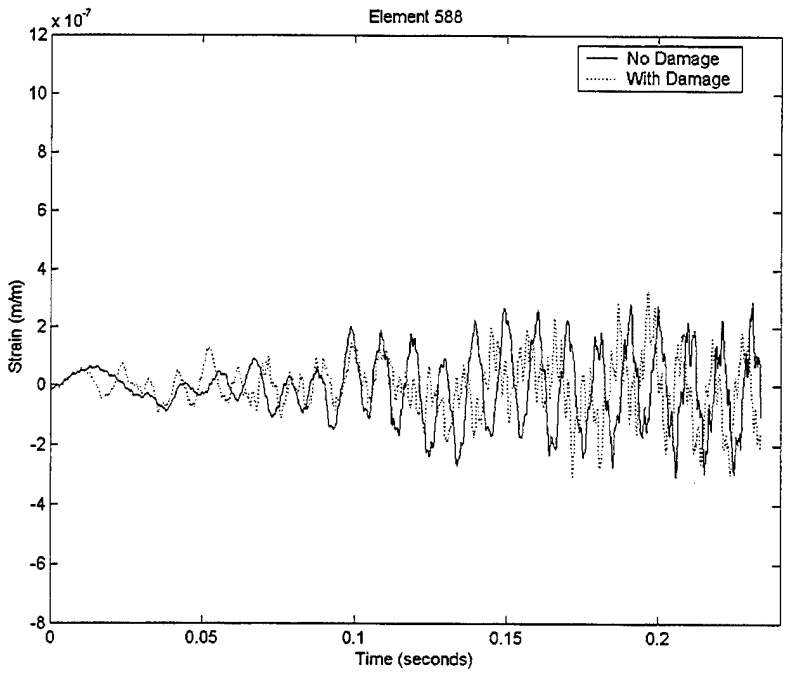

Figure 10a. Strain 0.02m Left of the Left Crack Tip, Element 588 (0.218 – 0.220m), Case 1 (0.24 – 0.25)

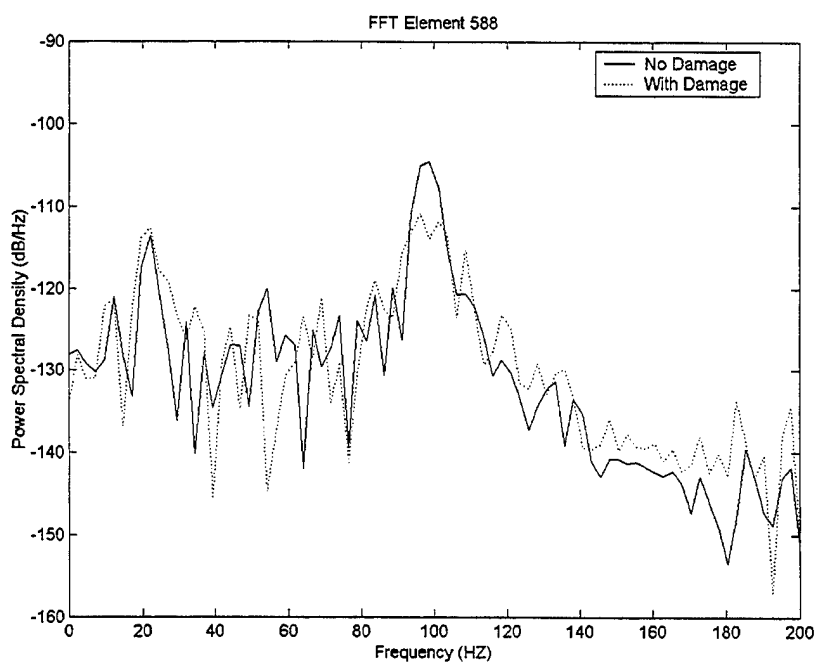

Figure 10b. PSD 0.02 m Left of the Left Crack Tip, Element 588 (0.218 – 0.220m), Case 1 (0.24 – 0.25)

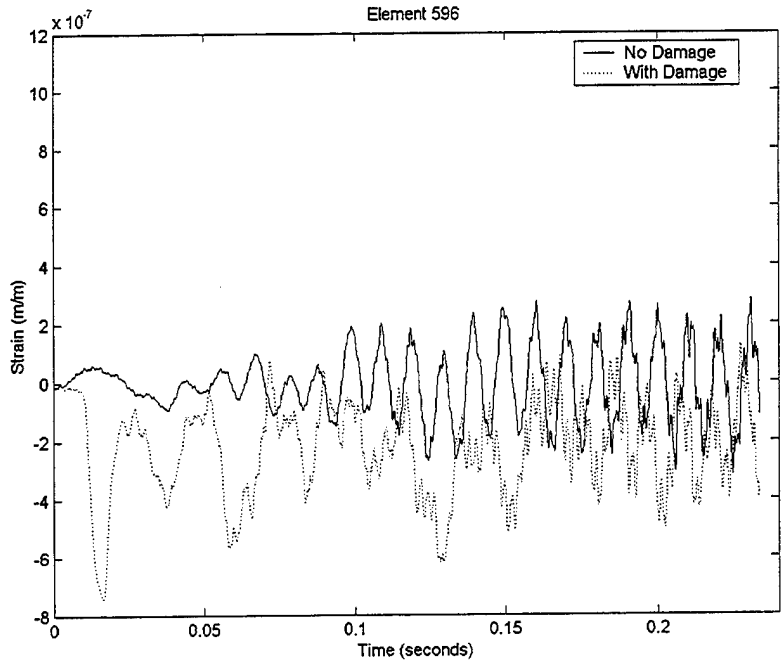

Figure 11a. Strain 0.004m Left of the Left Crack Tip, Element 596 (0.234 – 0.236), Case 1 (0.24 – 0.25)

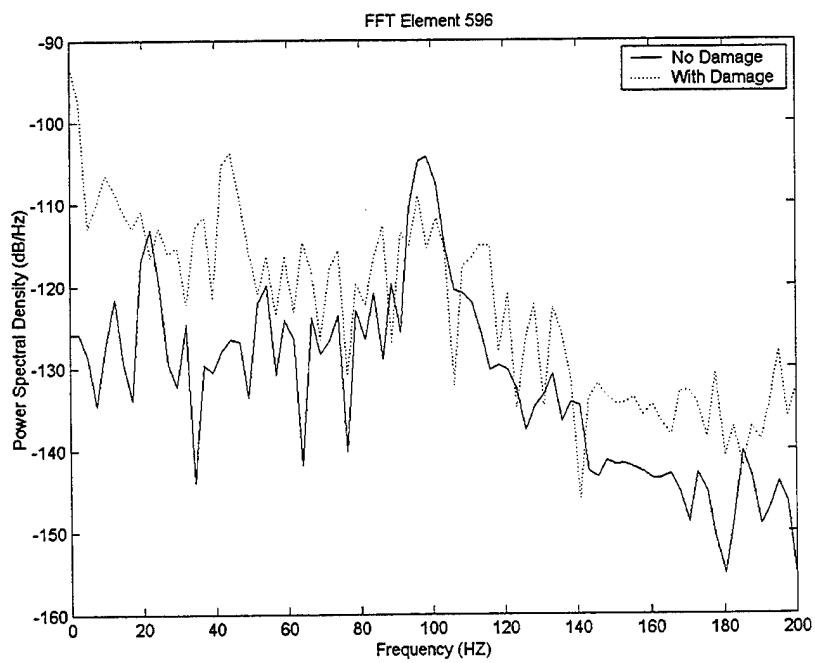

Figure 11b. PSD 0.004m Left of the Left Crack Tip, Element 596 (0.234 – 0.236), Case 1 (0.24 – 0.25)

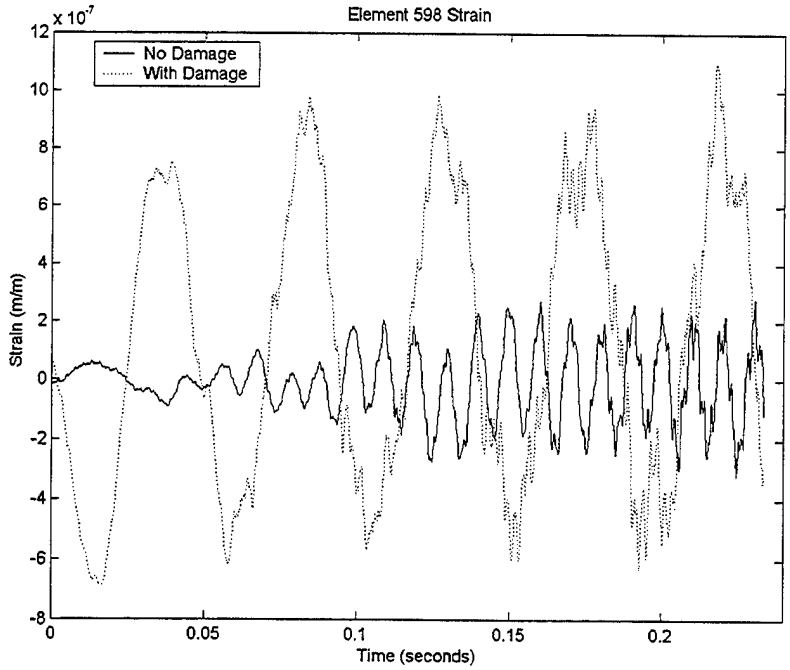

Figure 12a. Strain First Element Left of the Left Crack Tip, Element 598 (0.238 – 0.240m), Case 1 (0.24 – 0.25m)

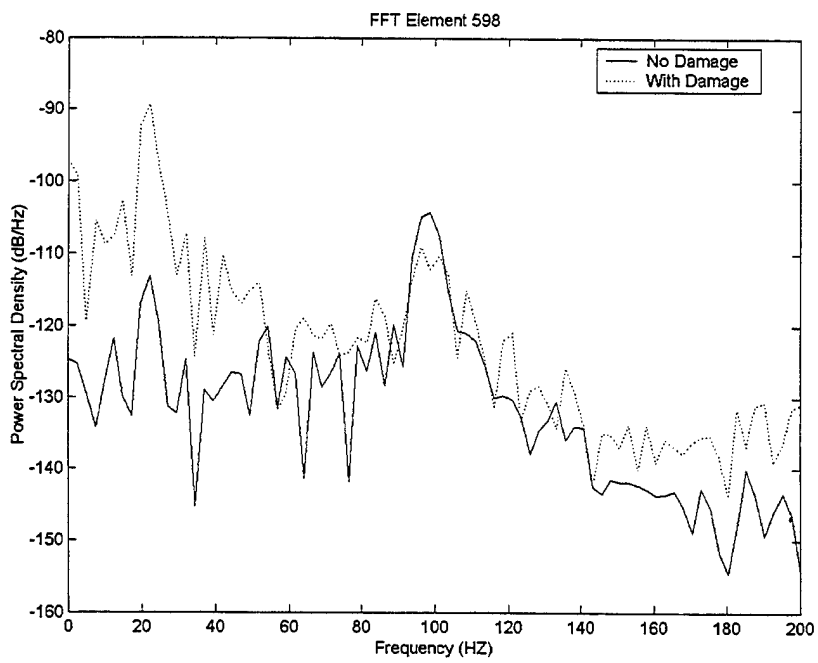

Figure 12b. PSD First Element Left of the Left Crack Tip, Element 598 (0.238 – 0.240m), Case 1 (0.24 – 0.25m)

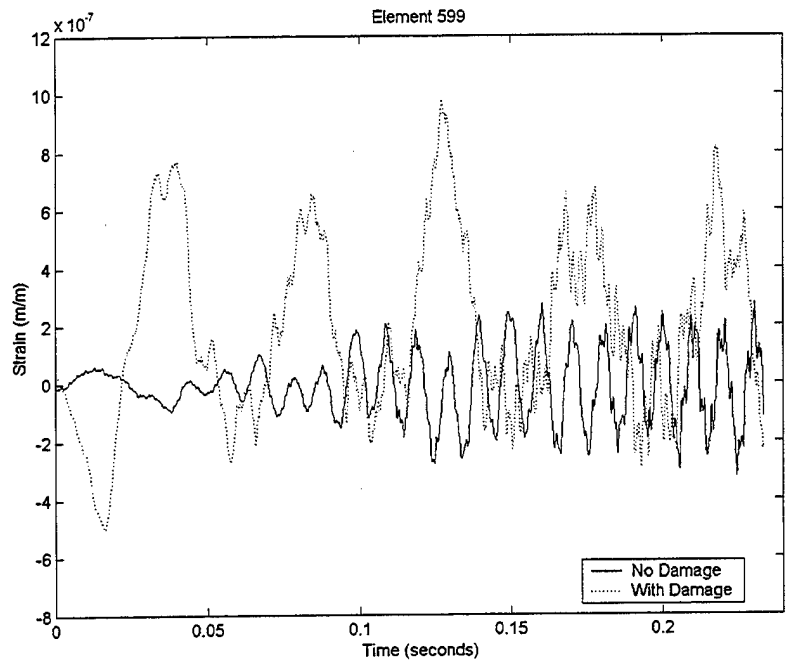

Figure 13a. Strain at Left Crack Tip, Element 599 (0.240 – 0.242m), Case 1 (0.24 – 0.25m)

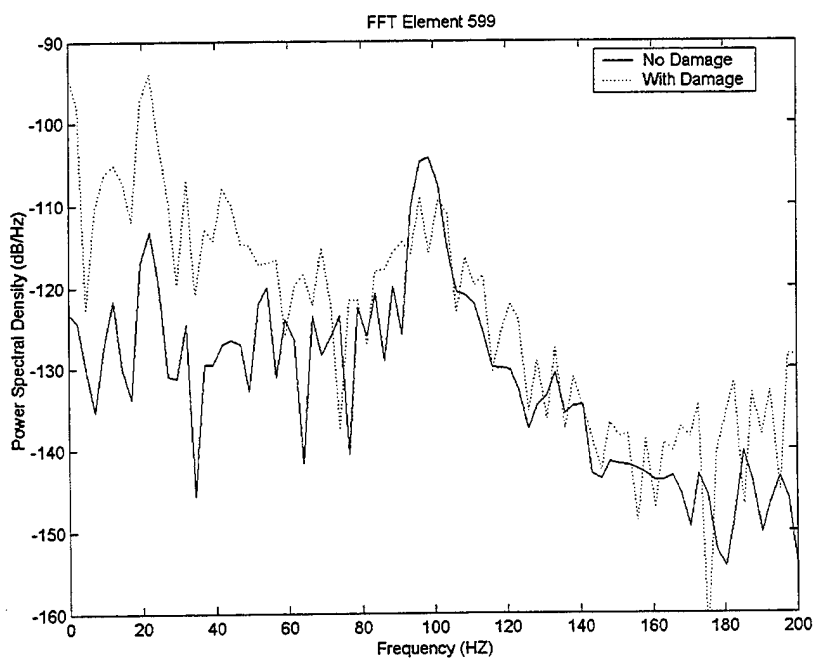

Figure 13b. PSD at Left Crack Tip, Element 599 (0.240 – 0.242m), Case 1 (0.24 – 0.25m)

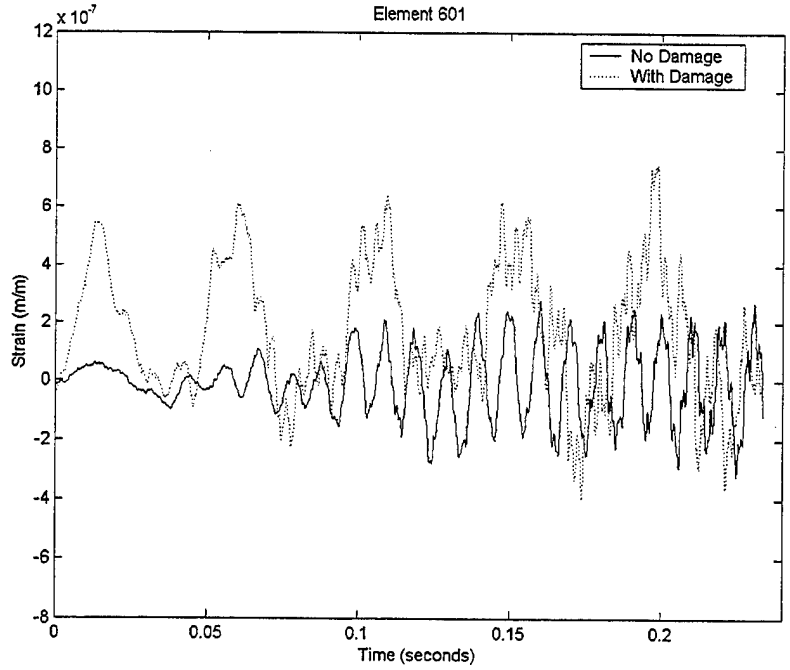

Figure 14a. Strain Inside the Crack, Element 601 (0.244 – 0.246m), Case 1 (0.24 – 0.25m)

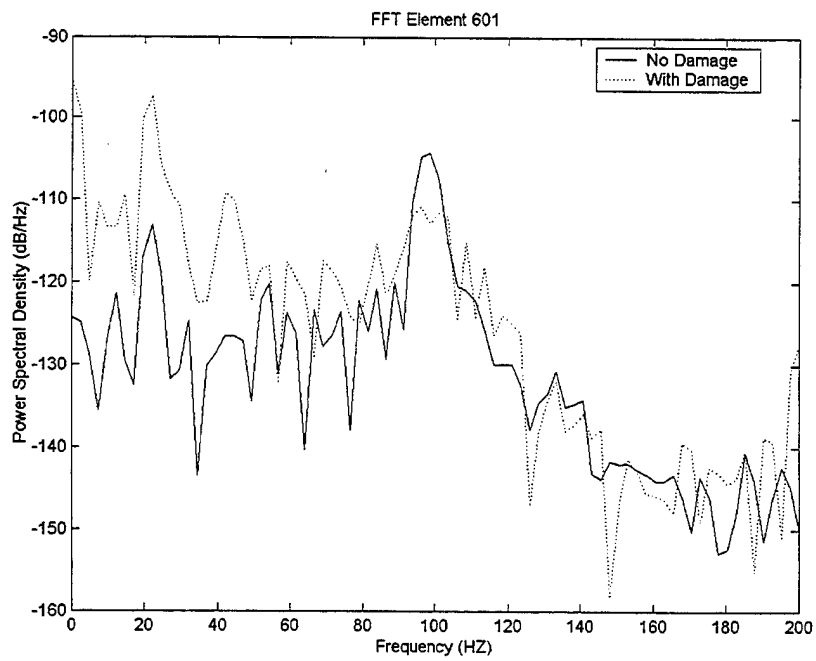

Figure 14b. PSD Inside the Crack, Element 601 (0.244 – 0.246m), Case 1 (0.24 – 0.25m)

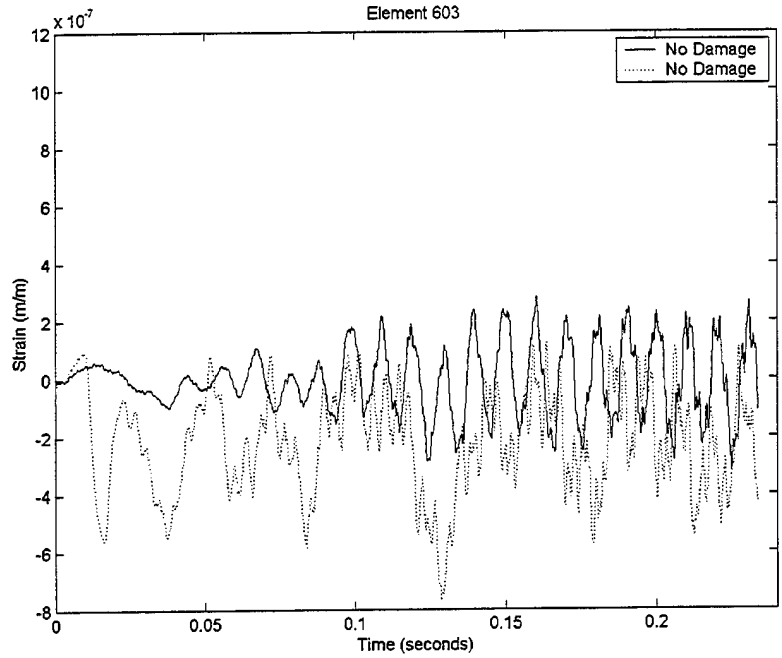

Figure 15a. Strain at the Right Crack Tip, Element 603 (0.248 – 0.250m), Case 1 (0.24 – 0.25m)

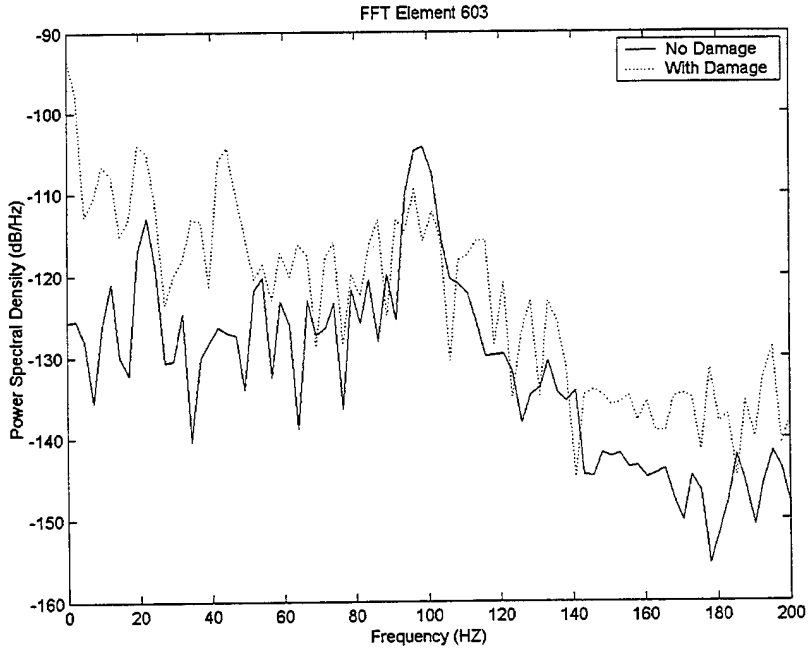

Figure 15b. PSD at the Right Crack Tip, Element 603 (0.248 – 0.250m), Case 1 (0.24 – 0.25m)

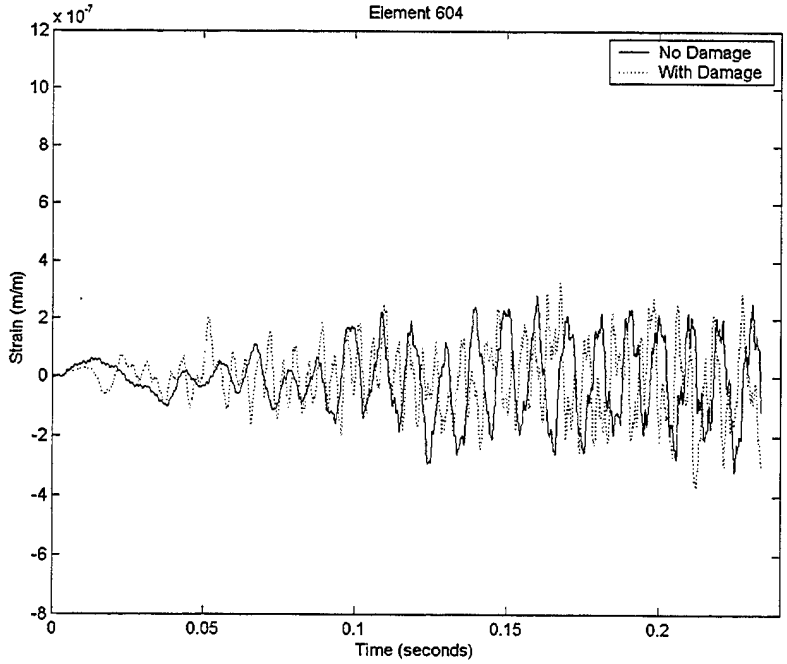

Figure 16a. Strain First Element Right of the Right Crack Tip, Element 604 (0.250 – 0.252m), Case 1 (0.24 – 0.25m)

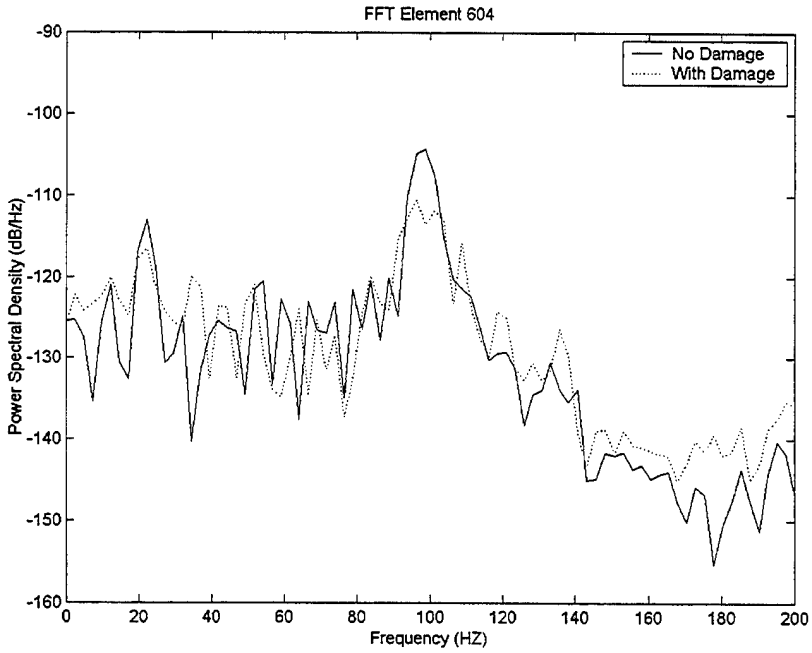

Figure 16b. PSD Strain First Element Right of the Right Crack Tip, Element 604 (0.250 – 0.252m), Case 1 (0.24 – 0.25m)

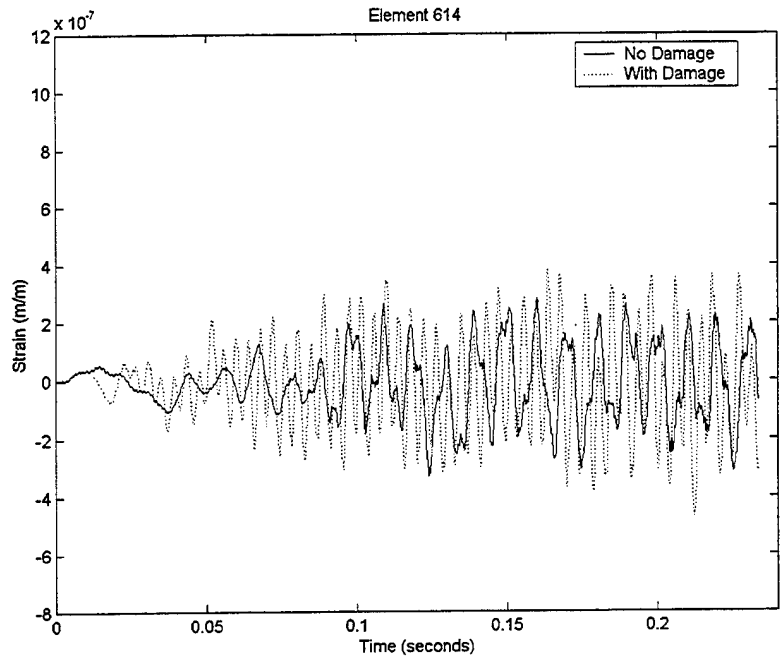

Figure 17a. Strain 0.02m Right of the Right Crack Tip, Element 614 (0.270 – 0.272m), Case 1 (0.24 – 0.25m)

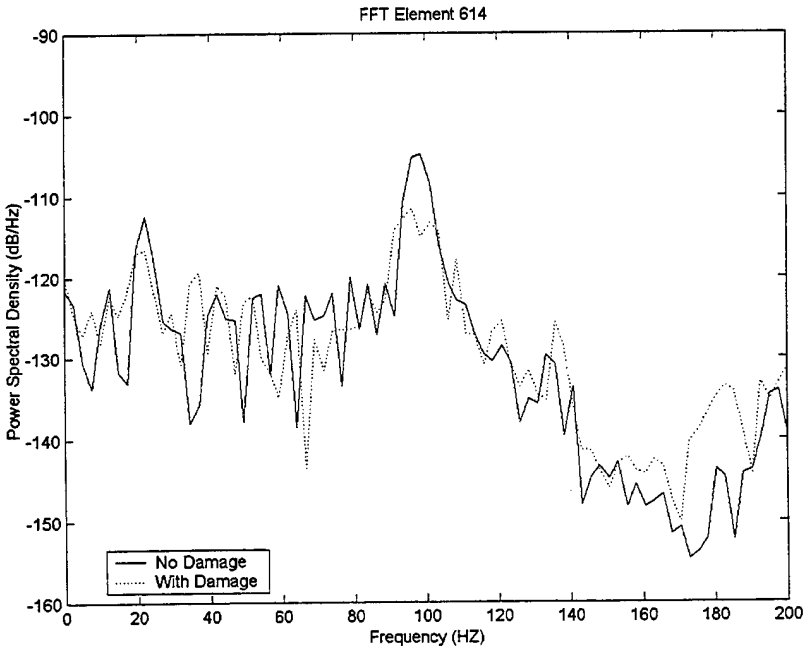

Figure 17b. PSD 0.02m Right of the Right Crack Tip, Element 614 (0.270 – 0.272m), Case 1 (0.24 – 0.25m)

b. Case 2: Interfacial Crack between 0.0 – 0.01 meters

As previously discussed, the effect of the clamped support overshadows the effect of the damage and the crack is undetectable. As summarized in Table 4, along with Figures 18 through 22, the strain and FFT plots do not show any effects of the damage. This implies that there exists an optimum crack detection range in relation to the support. Conversely, the expected location of damage in any structure is near the supports, so traditional methods of NDE are already in use in those locations. It is interesting to note that well away from the damaged section, as illustrated by Figures 21 and 22, the FEM does detect the presence of damage somewhere in the model, which is useful information.

Table 4. Case 2 FEM Interface Crack Detection Results

Element location	Damage Location	Figure/Element	Detection Probability
0.000 – 0.002m	0.00 – 0.01m	18/479	Low
0.004 – 0.006m	0.00 – 0.01m	19/481	Low
0.010 – 0.012m	0.00 – 0.01m	20/484	Low
0.034 – 0.036m	0.00 – 0.01m	21/496	High
0.042 – 0.044m	0.00 – 0.01m	22/500	High

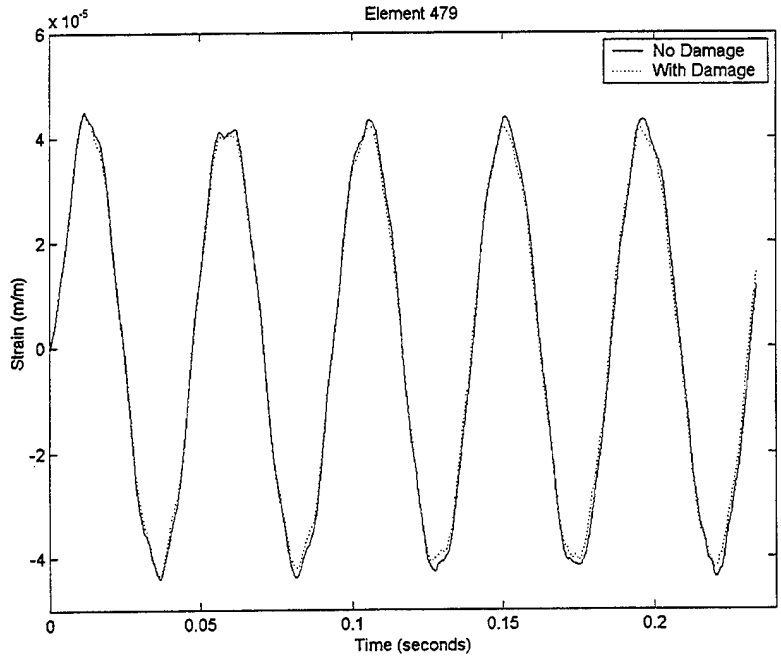

Figure 18a. Strain at the Left Crack Tip (and Clamped Support), Element 479 (0.0 – 0.002m) Case 2 (0.0 – 0.01m)

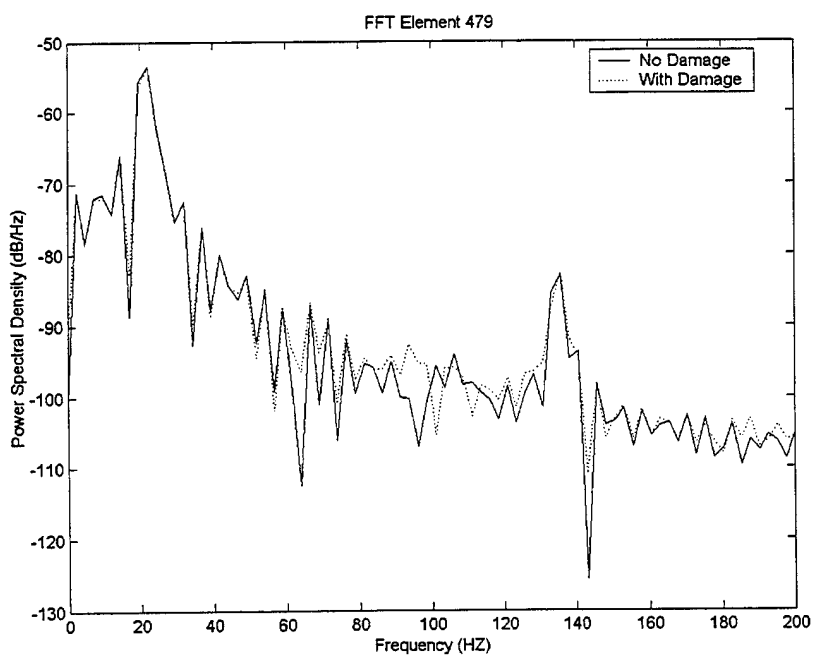

Figure 18b. PSD at Left Crack Tip (and Clamped Support), Element 479 (0.0 – 0.002m) Case 2 (0.0 – 0.01m)

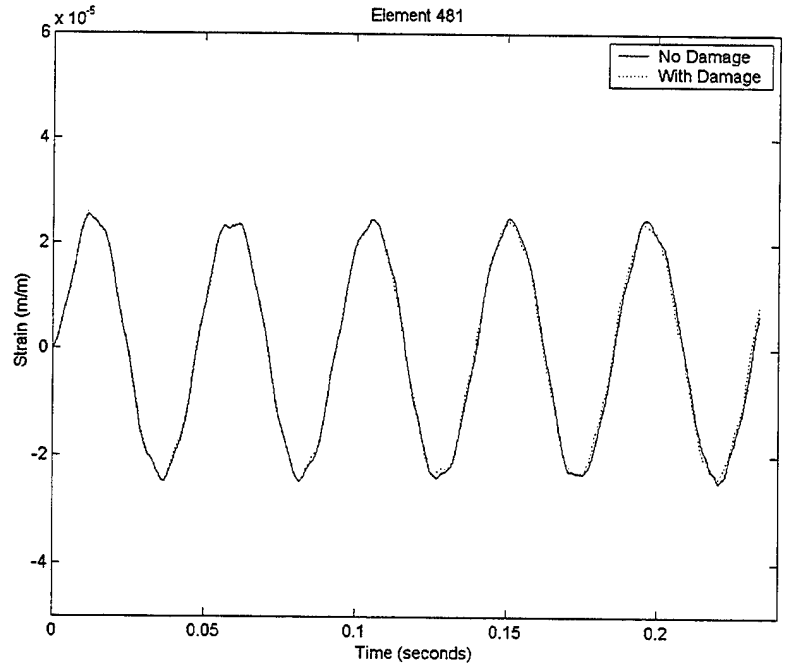

Figure 19a. Strain Inside the Crack, Element 481 (0.004 – 0.006m), Case 2 (0.0 – 0.01m)

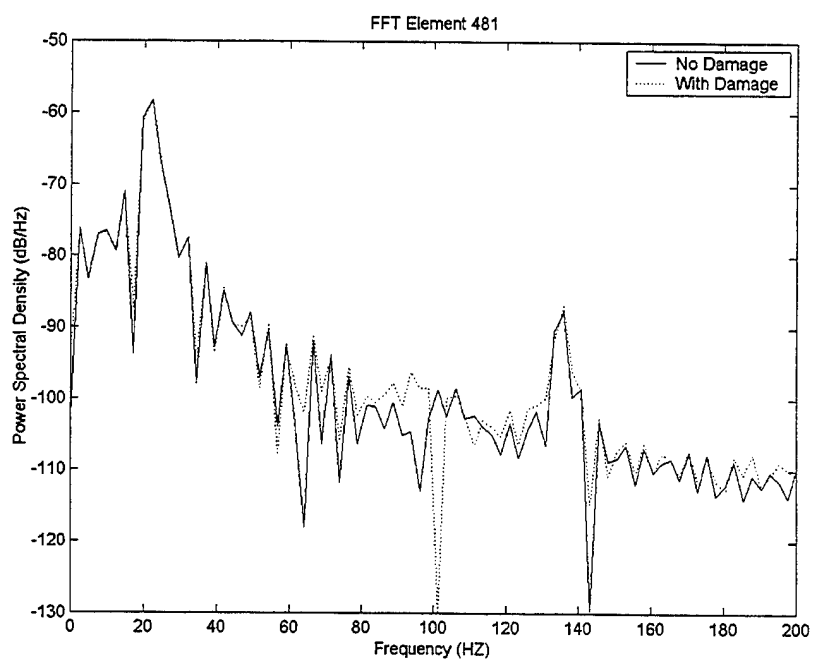

Figure 19b. PSD Inside the Crack, Element 481 (0.004 – 0.006m), Case 2 (0.0 –0.01m

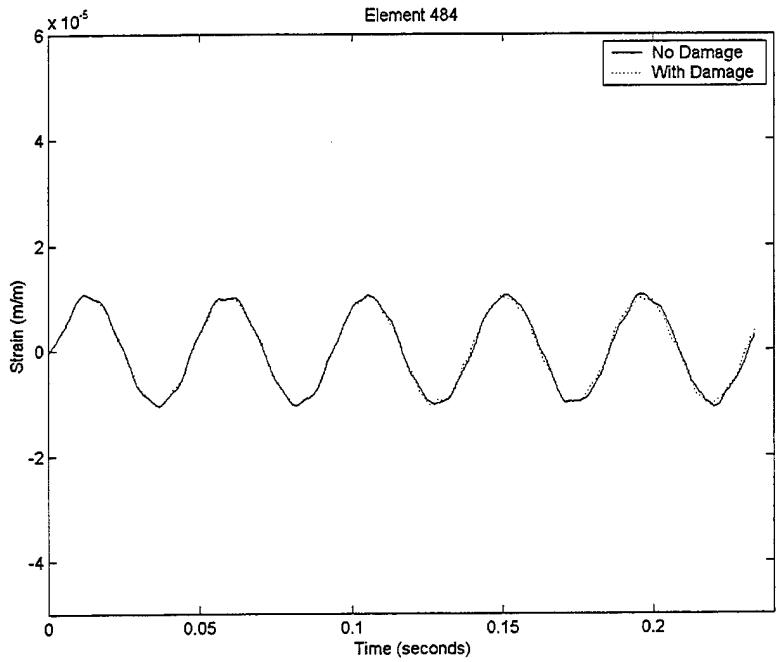

Figure 20a. Strain First Element Right of the Right Crack Tip, Element 484 (0.01 – 0.012m) Case 2 (0.0 – 0.01m)

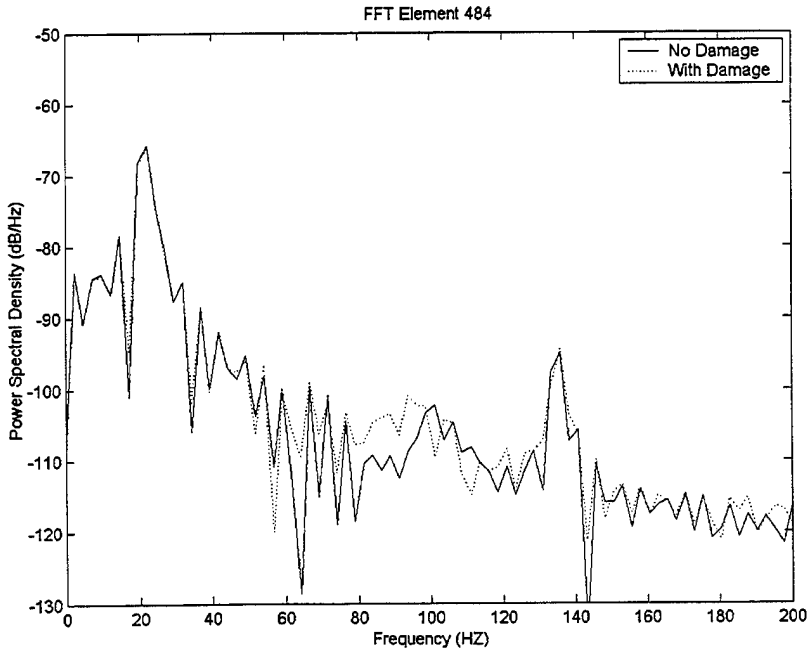

Figure 20b. PSD Strain First Element Right of the Right Crack Tip, Element 484 (0.01 – 0.012m) Case 2 (0.0 – 0.01m)

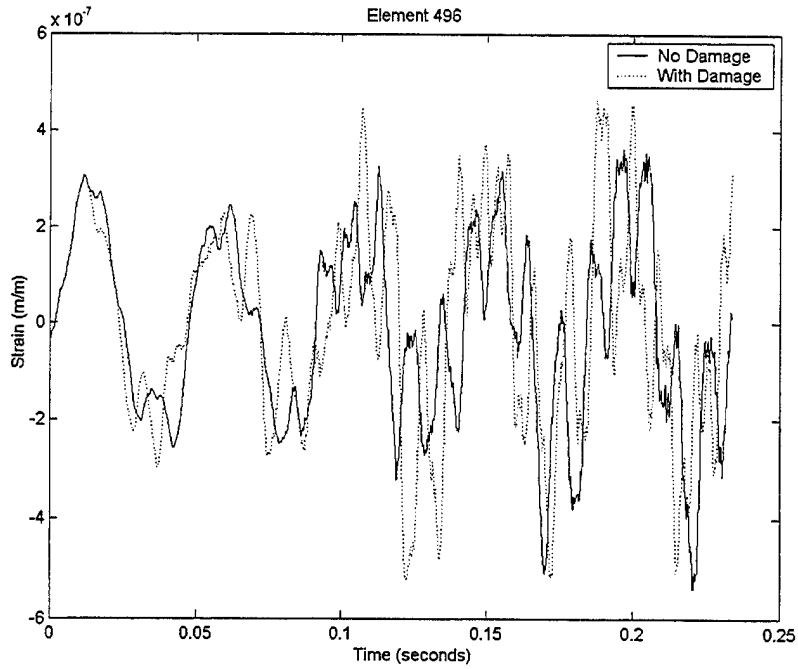

Figure 21a. Strain 0.024m Right of the Right Crack Tip, Element 496 (0.034 – 0.036m), Case 2 (0.0 – 0.01m)

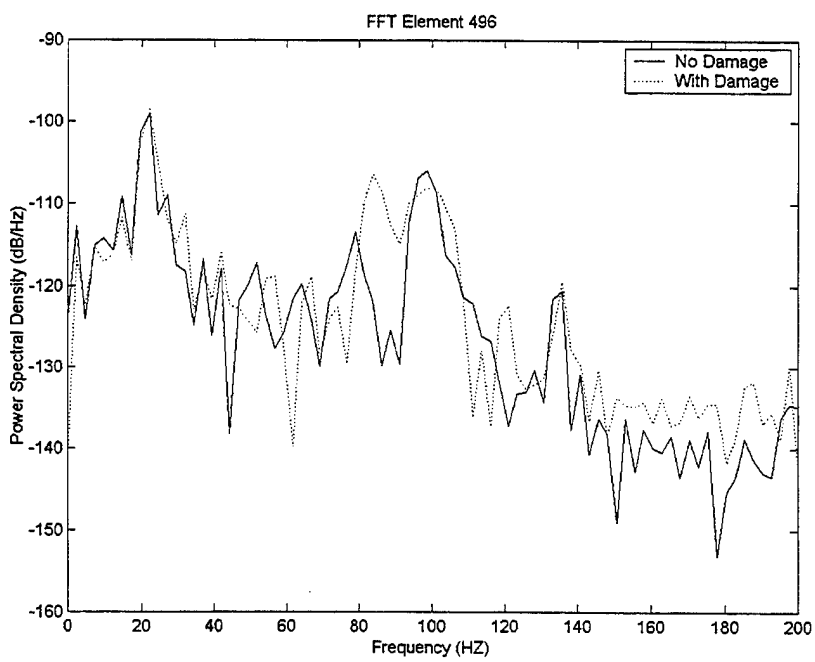

Figure 21b. PSD 0.024 m Right of the Right Crack Tip, Element 496 (0.034 – 0.036m), Case 2 (0.0 – 0.01m)

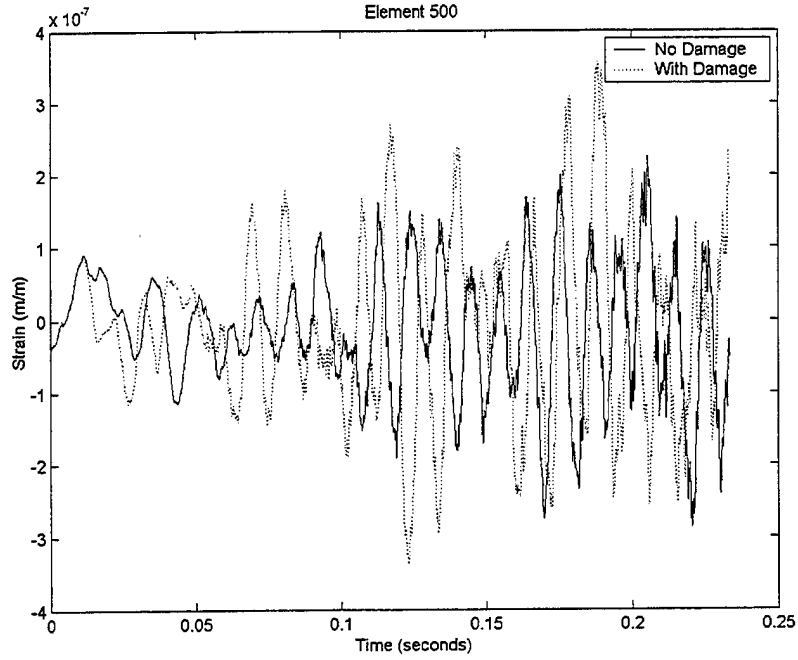

Figure 22a. Strain 0.032 m Right of the Right Crack Tip, Element 500 (0.042 – 0.044m), Case 2 (0.0 – 0.01m)

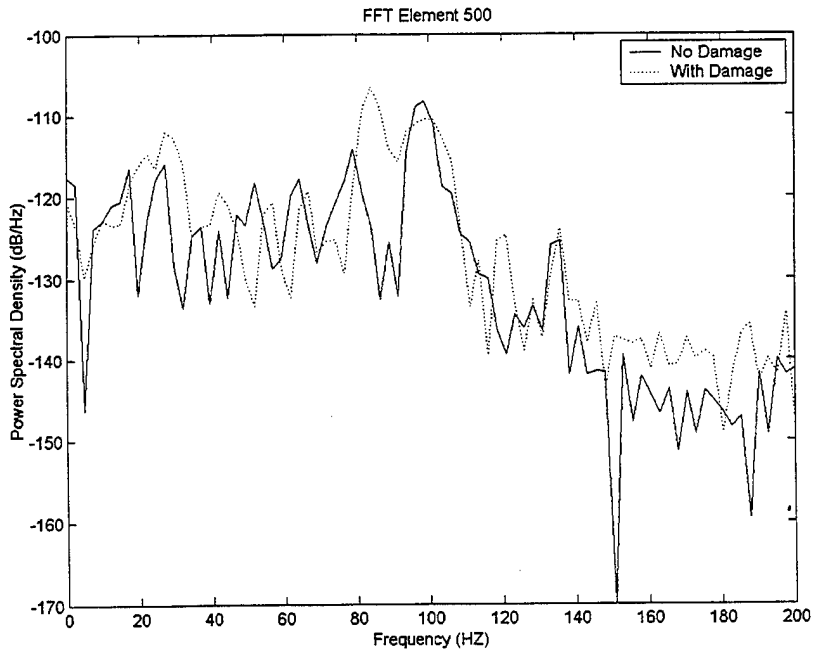

Figure 22b. PSD 0.032 m Right of the Right Crack Tip, Element 500 (0.042 – 0.044m), Case 2 (0.0 – 0.01m)

c. *Case 3: Interfacial Crack between 0.01 – 0.02 meters*

Unlike Case 2, a short distance from the clamped support, the effects of the interfacial crack are readily detectable. However, analysis of the elements between the clamped support and the interfacial crack, does not indicate the presence of damage, which is masked by the nearness of the clamped support. The effects of damage are not seen by the model until very close to the actual damage, which supports the notion of using the FEM as a damage location predictor device. Table 5, along with Figures 23 through 27, summarizes the probability of damage detection.

At Element 489, Figure 24 (Left Crack Tip) there is actually a decrease in elemental strain compared to the undamaged beam, although there is a slight frequency increase. Once inside the crack itself, the damage manifests itself as generally compressive strains that are actually less than the undamaged case. Conversely, the tensile strains are typically higher in magnitude. Element 493, Figure 26 (Right Crack Tip) shows a dramatic increase in compressive elemental strains compared to Element 491, Figure 25. Conversely, Element 491 has higher tensile strains than Element 493. The effect of the crack is very clear when compared to neighboring elements and this effect is limited to the area of the crack. The crack effect does not grow or spill over to neighboring elements as seen in Case 1. Again, this implies that there exists an optimum crack detection range in relation to the support.

Table 5. Case 3 FEM Interface Crack Detection Results

Element Location	Damage Location	Figure/Element	Detection Probability
0.018 – 0.020m	0.020 –0.030m	23/488	High
0.020 –0.022m	0.020 –0.030m	24/489	High
0.024 – 0.026m	0.020 –0.030m	25/491	High
0.028 – 0.030m	0.020 –0.030m	26/493	High
0.234 – 0.236m	0.020 –0.030m	27/596	Low

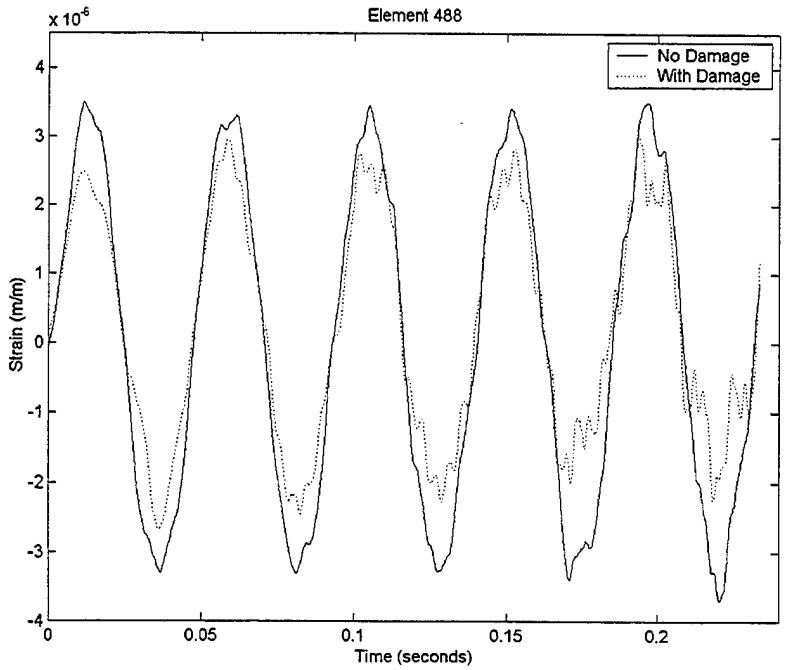

Figure 23a. Strain First Element Left of the Left Crack Tip, Element 488 (0.018 – 0.02m), Case 3 (0.02 – 0.03m)

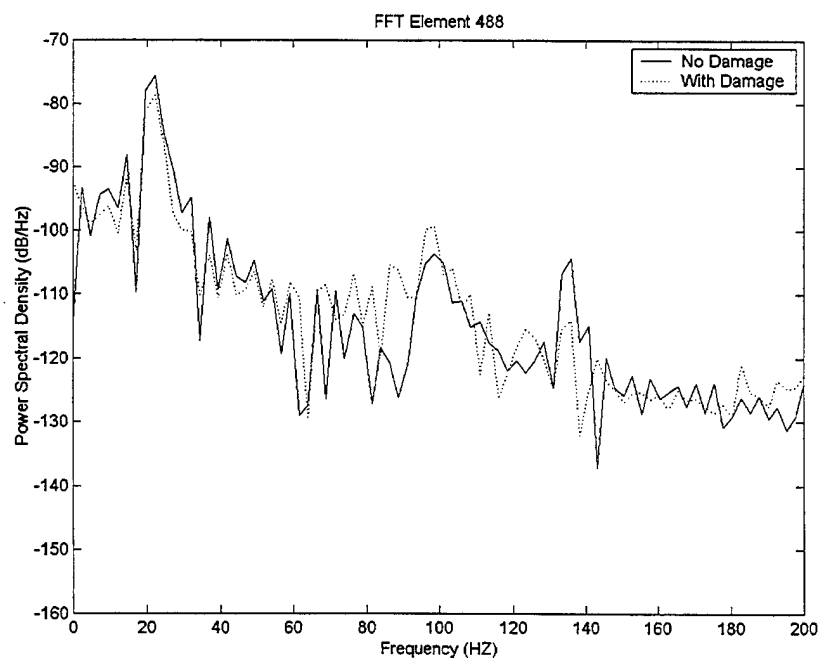

Figure 23b. PSD First Element Left of the Left Crack Tip, Element 488 (0.018 – 0.02m), Case 3 (0.02 – 0.03m)

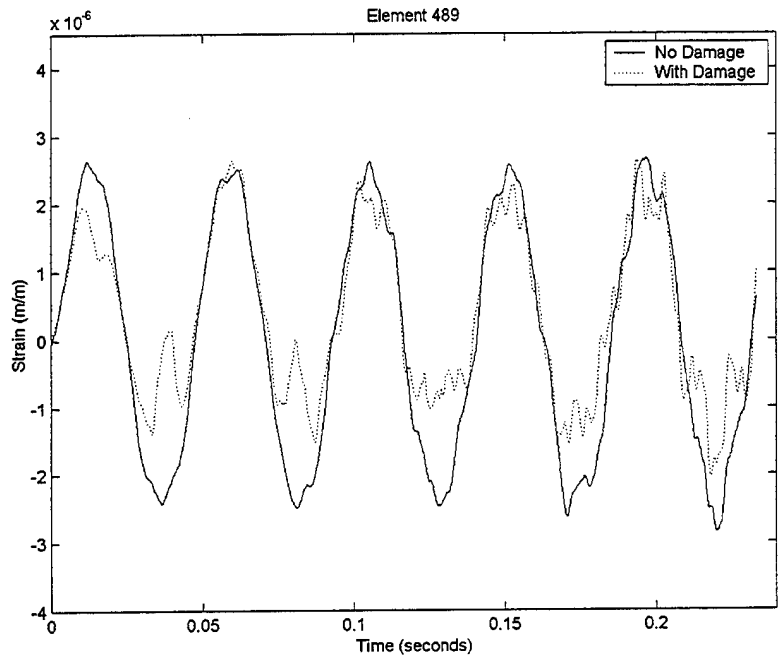

Figure 24a. Strain at the Left Crack Tip, Element 489 (0.02 – 0.022m), Case 3 (0.02 – 0.03m)

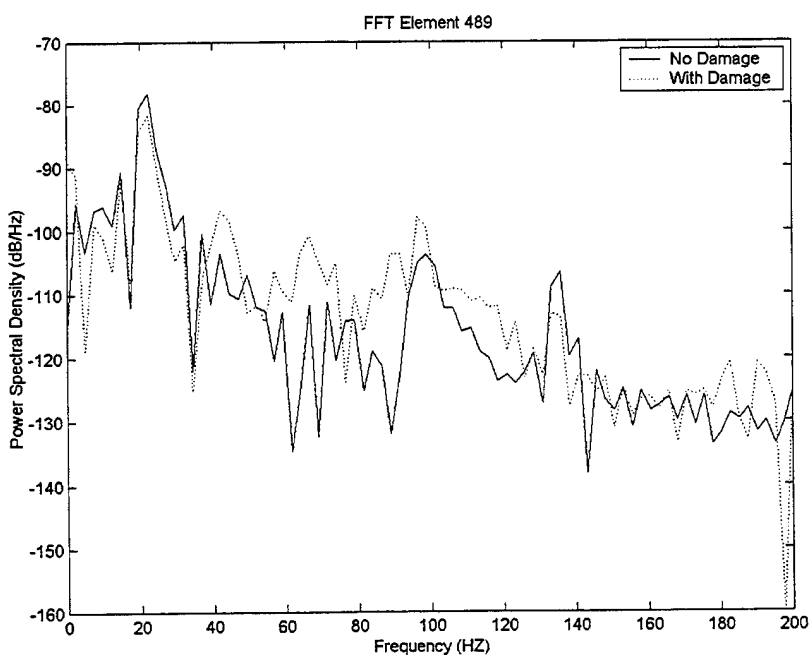

Figure 24b. PSD at the Left Crack Tip, Element 489 (0.02 – 0.022m), Case 3 (0.02 – 0.03m)

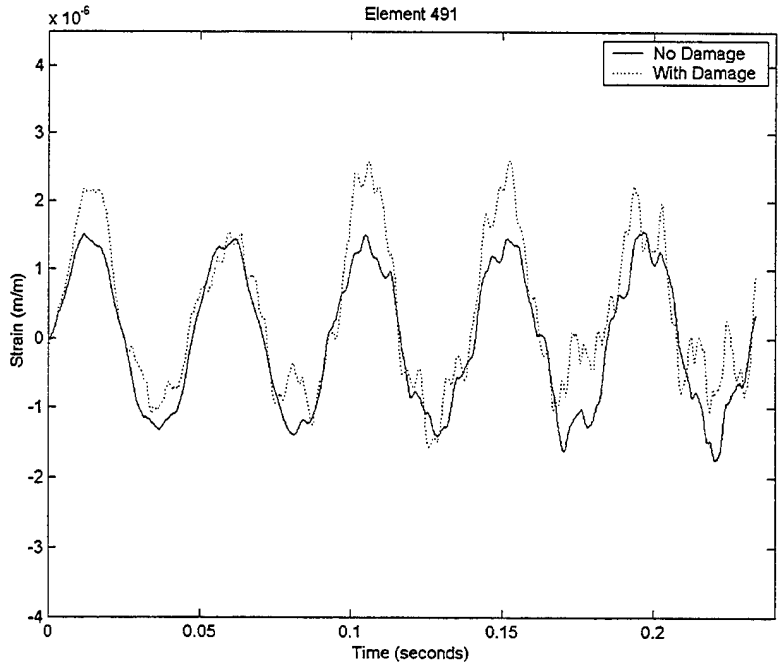

Figure 25a. Strain Inside the Crack, Element 491 (0.024 – 0.026m), Case 3 (0.02 – 0.03m)

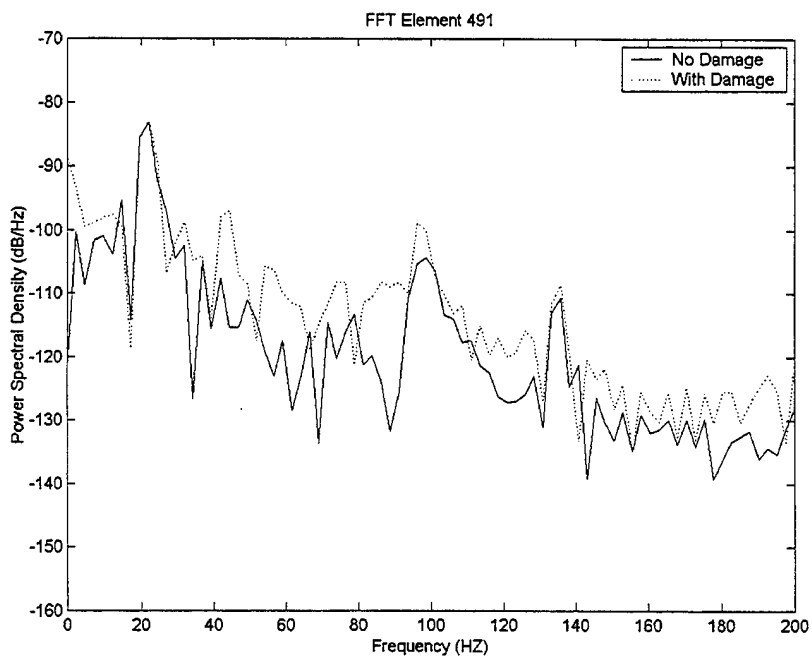

Figure 25b. PSD Inside the Crack, Element 491 (0.024 – 0.026m), Case 3 (0.02 – 0.03m)

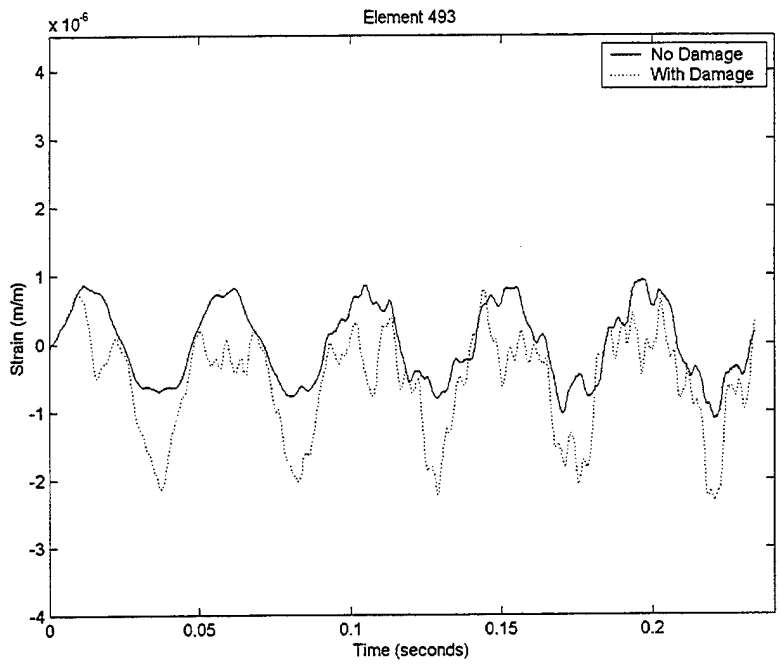

Figure 26a. Strain at the Right Crack Tip, Element 493 (0.028 – 0.03m), Case 3 (0.02 – 0.03m)

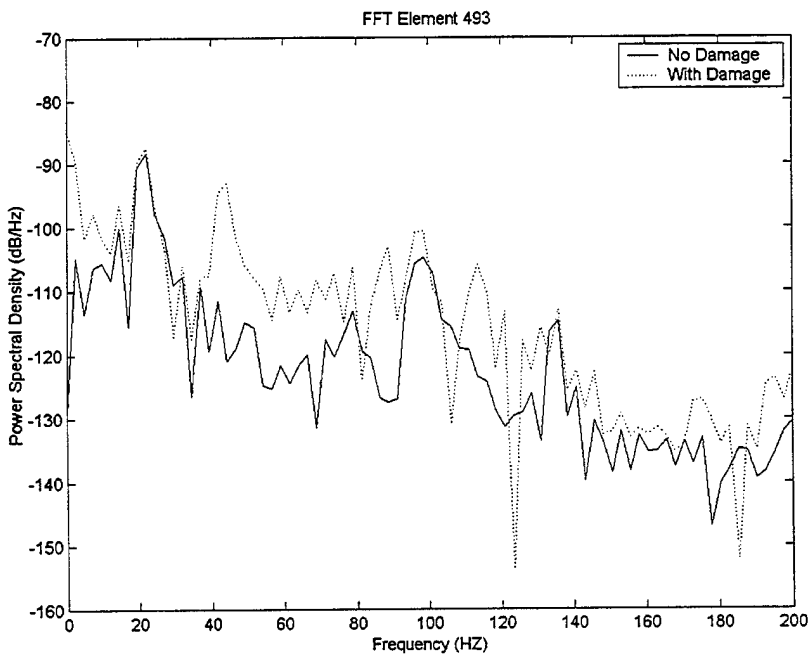

Figure 26b. PSD at the Right Crack Tip, Element 493 (0.028 – 0.03m), Case 3 (0.02 – 0.03m)

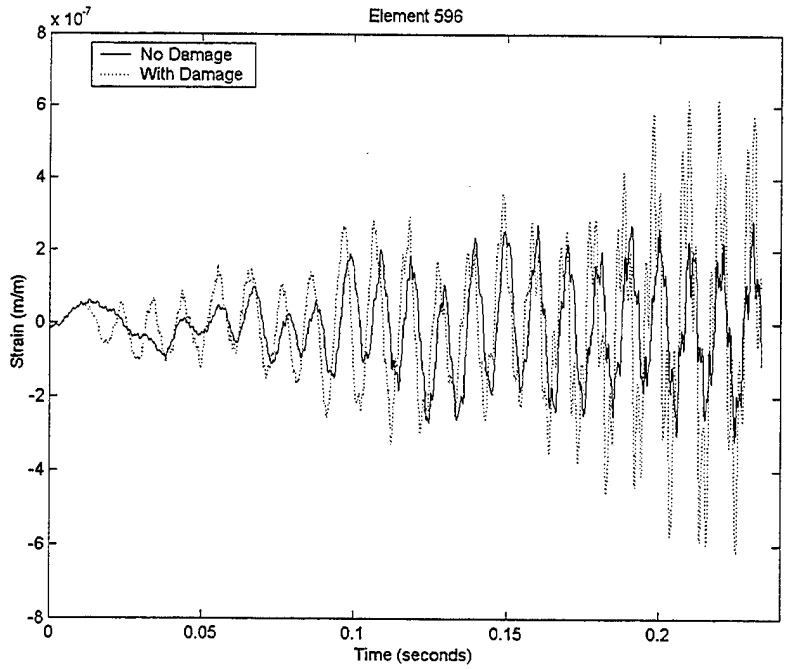

Figure 27a. Strain 0.004m Right of the Right Crack Tip, Element 596 (0.234 – 0.236m), Case 3 (0.02 – 0.03m)

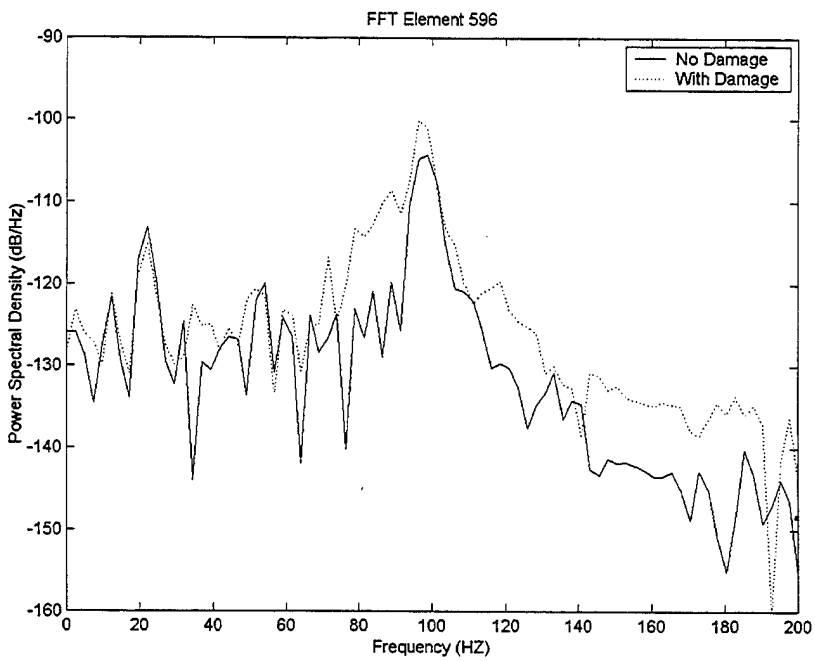

Figure 27b. PSD 0.004 m Right of the Right Crack Tip, Element 596 (0.234 – 0.236m), Case 3 (0.02 – 0.03m)

B. SIMPLY SUPPORTED SANDWICH COMPOSITE PLATE

1. Effects of Contact Elements

Two different sized interfacial cracks were modeled in the simply supported plate. The first case was a 0.01m by 0.01m crack centered about X = 0.21m and Z = 0.23m, and the second case was a 0.03m by 0.03m crack centered about X = 0.22m and Z = 0.22m. In both cases an impact load of 1 N was applied at X = 0.27m and Z = 0.17m, and a run time of 0.025 seconds was used in both instances.

The first case was modeled without contact elements, and thus without friction, but the FEM was unable to differentiate the interfacial crack from the undamaged case. This is contrary to the cantilever beam cases. The second case was developed using contact elements and an interfacial crack that was three times larger than the Case 1. Two versions of Case 2 were modeled, one with friction and the other without. However, both cases diverge at approximately 0.006 and 0.003 seconds, respectively.

Various attempts were made to correct this obvious shortcoming in this analysis but to no avail. The best solution for the divergence issue was to eliminate the use of the contact elements. That was considered a non-solution since the cantilevered beam analysis clearly demonstrated their importance and since the FEM was unable to detect the crack.

Figures 28 and 29 illustrate that the FEM diverges when contact elements are used, for the 0.01m by 0.01m interfacial crack.

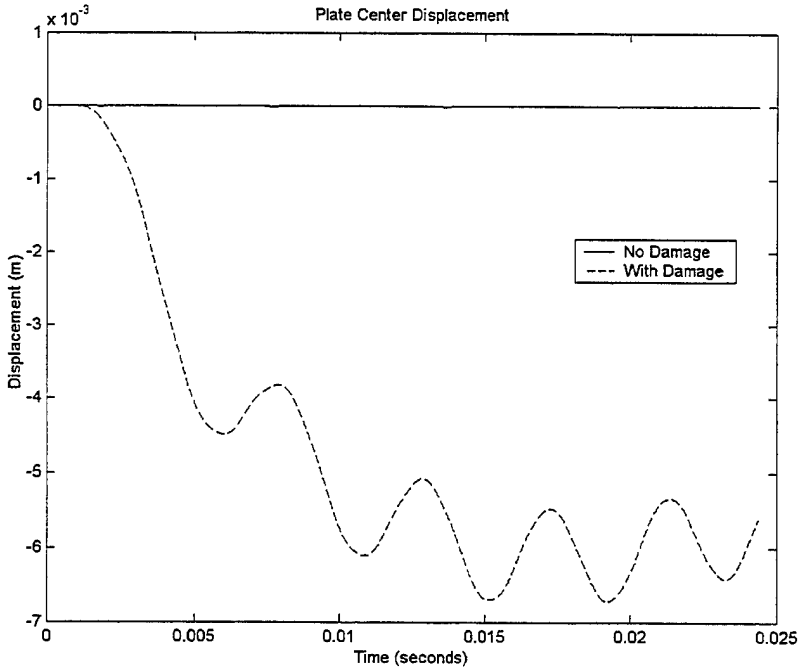

Figure 28. Center Displacement Divergence of the Plate with 0.01m by 0.01m Interfacial Crack with Contact Elements and Zero Friction.

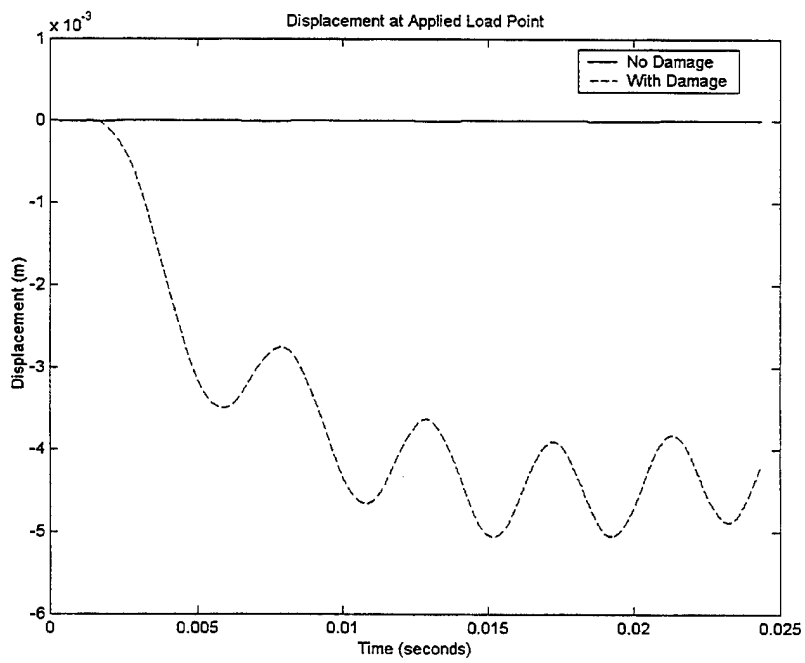

Figure 29. Load Point Displacement Divergence of the Plate with 0.01m by 0.01m Interfacial Crack with Contact Elements and Zero Friction

Likewise for the plate with the larger, 0.03m by 0.03m, damaged section, if contact elements are used the FEM also diverges. However, without using contact elements in the model, the presence of the crack can not be detected, as illustrated by Figure 30.

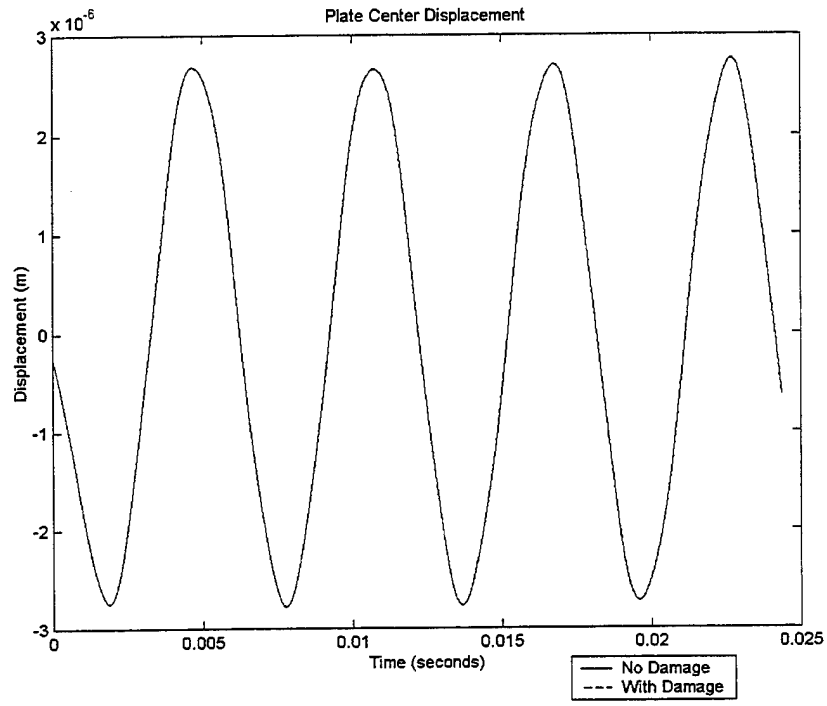

Figure 30. Center Displacement of the Plate with 0.03m by 0.03m Interfacial Crack but without Contact Elements

THIS PAGE INTENTIONALLY LEFT BLANK

V. CONCLUSIONS AND RECOMMENDATIONS

A. CONCLUSIONS

This research has clearly demonstrated that in order to improve the accuracy and realism of the FEM, the use of contact elements, and thus non-linear analysis is required. The effects and therefore the values employed for the coefficients to friction are less significant. The FEM can readily be used to predict and localize the presence of an interfacial crack through strain measurements. The existence of damage at the clamped support is masked by the clamped support of the cantilever beam. Unfortunately, the plate bending problem, with contact elements, at the interface crack exhibited instability. The plate-bending problem without the use of contact elements was unable to detect the damaged sections.

B. RECOMMENDATIONS

1. Correlation

The FEM must be validated by direct comparison to an experimental configuration. Park et al (1999) offers an example of an experimental apparatus using fiber-optic strain gages that could be used as a validation tool. The FEM could then be optimized to match the experimental results.

2. FEM Plate and Cylinder geometry

It is very unfortunate that this research was unable to achieve valid results with the simply supported plate FEM. It was hoped that the plate model would have been used as a springboard to more complex geometry such as a cylinder or sphere. Obviously, until the FEM can solve the two-dimensional plate-bending problem, it cannot be used for problems that are more complex.

3. FEM program limitations

In its current configuration, further research is hampered by the use of DYNA3D without a pre or post-processor. A lot of time is required to build simple models and far more time is spent in data analysis using MATLAB. Presently, on a SGI Octane workstation, the beam models require approximately 130 hours of computation time. Clearly, this computation time is excessive such basic geometry. If this work is to continue, then either a different program or additional software, in the form of a pre- and post-processor, are necessary.

LIST OF REFERENCES

Chance, J., G.R. Tollinson, and K. Worden (1994). *"A Simplified Approach to the Numerical and Experimental Modeling of Dynamics of a Cracked Beam,"* Proc of the 12th International Modal Analysis Conference, Honolulu, Hawaii, Vol. I, pp. 778-785.

Chang, F.-K., (1999), *"Structural Health Monitoring: A summary Report on the First International Workshop on Structural Health Monitoring, September 18-20, 1997,"* Proceedings of the 2nd International Workshop on Structural Health Monitoring: Current Status and Perspectives, Fu-Kuo Chang, ed., Technomic Publishing Company, Lancaster PA, pp. xix – xxix.

Doebling, S.W., C.R., Farrar, M.B., Prime, and D.W., Shevitz, (1996) *"Damage Identification and Health Monitoring of Structural and Mechanical Systems from Changes in Their Vibration Characteristics: A Literature Review,"* Los Alamos National Laboratory Report LA-13070-MS, Los Alamos, New Mexico.

Farrar, C.R and D.V., Jauregui, (1996a) *"Damage Detection Algorithms Applied to Experimental and Numerical Modal Data from the I-40 Bridge,"* Los Alamos National Laboratory Report LA-13074-MS, Los Alamos, New Mexico.

Farrar, C.R., T.A., Duffey, P.A., Goldman, D.V., Jauregui, and J.S., Vigil, (1996b) *"Finite Element Analysis of the I-40 Bridge over the Rio Grande,"* Los Alamos National Laboratory Report LA-12979-MS, Los Alamos, New Mexico.

Farrar, C.R., and S.W., Doebling, (1997), *"Lessons Learned from Applications of Vibration-Based Damage Identification Methods to a Large Bridge Structure,"* Proceedings of the 1st International Workshop on Structural Health Monitoring: Current Status and Perspectives, Fu-Kuo Chang, ed., Technomic Publishing Company, Lancaster PA, pp. 351 - 370.

Foote, P.D., (1999), *"Structural Health Monitoring: Tales From Europe,"* Proceedings of the 2nd International Workshop on Structural Health Monitoring: Current Status and Perspectives, Fu-Kuo Chang, ed., Technomic Publishing Company, Lancaster PA, pp. 24 - 35.

Hallquist, J., and D.W., Stillman, (1990), *"VEC/DYNA3D User's Manual for Nonlinear Dynamic Analysis of Structures in Three Dimensions,"* Livermore Software Technology Corporation, Livermore, CA.

Helnicki, A, J., A.E., Attain, L.K., Comfort, and M., Kam, (1997), *"Information Technology in Civil Infrastructure System Monitoring: Opportunities and Issues,"* Proceedings of the 1st International Workshop on Structural Health Monitoring: Current Status and Perspectives, Fu-Kuo Chang, ed., Technomic Publishing Company, Lancaster PA, pp. 396 - 409.

Ikagami, R., (1999), *"Structural Health Monitoring: Assessment of Aircraft Customer Needs,"* Proceedings of the 2nd International Workshop on Structural Health Monitoring: Current Status and Perspectives, Fu-Kuo Chang, ed., Technomic Publishing Company, Lancaster PA, pp. 12 - 23.

Lipsey, S. A., (1999), "*Numerical Study for Global Detection of Cracks Embedded in Beams,*" Master's Thesis, Naval Postgraduate School, Monterey, CA.

Mita, A., (1999), "*Immerging Needs in Japan for Health Monitoring Technologies in Civil and Building Structures,*" Proceedings of the 2nd International Workshop on Structural Health Monitoring: Current Status and Perspectives, Fu-Kuo Chang, ed., Technomic Publishing Company, Lancaster PA, pp. 56 - 67.

Park, J W., C.Y., Ryu, H.K., Kang, and C. S., Hong, (2000), "*Detection of Buckling and Crack Growth in the Delaminated Composites Using Fiber Optic Sensor,*" Journal of Composite Materials, Vol. 34, No. 19/2000, Technomic Publishing Company, Lancaster PA, pp. 56 - 67.

Seale, I., S., Ziola, and S., May, (1997), "*Damage Detection Experiments and Analysis for the F-16,*" Proceedings of the 1st International Workshop on Structural Health Monitoring: Current Status and Perspectives, Fu-Kuo Chang, ed., Technomic Publishing Company, Lancaster PA, pp. 310 - 324.

Sikorsky, C., (1999), "*Development of a Health Monitoring System for Civil Structures using a Level IV Non-Destructive Damage Evaluation Method,*" Proceedings of the 2nd International Workshop on Structural Health Monitoring: Current Status and Perspectives, Fu-Kuo Chang, ed., Technomic Publishing Company, Lancaster PA, pp. 68 - 81.

Rytter, A., (1993), "*Vibration Based Inspections of Civil Engineering Structures,*" Ph.D. Thesis, Department of Building Technology and Structural Engineering, Aalborg University, Denmark.

Valdiver, T. L., (1997), "*Health Monitoring of U.S. Army Missile Systems,*" Proceedings of the 1st International Workshop on Structural Health Monitoring: Current Status and Perspectives, Fu-Kuo Chang, ed., Technomic Publishing Company, Lancaster PA, pp. 191 - 196.

INITIAL DISTRIBUTION LIST

1. Defense Technical Information Center 2
   8725 John J. Kingman Road, Suite 0944
   Ft. Belvoir, VA 22060-6218

2. Dudley Knox Library 2
   Naval Postgraduate School
   411 Dyer Road
   Monterey, CA 93943-5101

3. Professor Young W. Kwon, Code ME/KW 2
   Naval Postgraduate School
   Monterey, CA 93943-5109

4. LT Daniel L. Lannamann, USN 3
   1421 Casa Grande
   Corpus Christi, TX 78411

5. Naval Engineering Curricular Office, Code 34 1
   Naval Postgraduate School
   700 Dyer Road
   Monterey, CA 93943-5109